(18 mM Tris base, 18 mM boric acid, and 0.4 mM EDTA). DNA was visualized by ethidium bromide staining.

Pull-down assay with GST-cFANCL and cFANCD2

Purified cFANCD2 (6 μg) and GST-cFANCL (5 μg) were incubated at 30°C for 60 min in a 100 μl reaction mixture, containing 20 mM Tris–HCl (pH 8.0), 10% glycerol, 200 mM NaCl, and 5 mM 2-mercaptoethanol. Glutathione Sepharose 4B beads (5 μl) were added to the reaction mixtures, which were gently mixed at 4°C for 60 min. The beads were then washed three times with 1 ml of wash buffer, containing 20 mM Tris–HCl (pH 8.0), 0.4 M NaCl, 10% glycerol, 5 mM 2-mercaptoethanol, and 0.05% Triton X-100. The proteins bound to the beads were separated by 7% SDS–PAGE, and were visualized by Coomassie Brilliant Blue staining.

In vitro FANCD2 monoubiquitination and purification of monoubiquitinated FANCD2

Experimental procedures are described in Supplementary Materials and Methods.

Gel-shift assay

Circular ϕX174 dsDNA (100 ng) was mixed with cFANCD2 (0.45–1.8 μM) or cFANCD2(1-1389) (0.45–1.8 μM) in 10 μl of reaction buffer, containing 22 mM Tris–HCl (pH 8.0), 70 mM NaCl, 7% glycerol, 2 mM $MgCl_2$, and 2.5 mM dithiothreitol. The samples were incubated at 37°C for 15 min, and were then analysed by 0.8% agarose gel electrophoresis in TAE buffer. DNA was visualized by ethidium bromide staining.

siRNA transfection, immunoblotting, and FRAP

The FANCD2-specific Stealth RNAs ((no. 1, HSS103525, 5′-AAUG AACGCUCUUUAGCAGACAUGG-3′, for Figures 3 and 6, and Supplementary Figure S3; and no. 2, HSS103527, 5′-AAUAGA CGACAACUUAUCCAUCACC-3′, for Supplementary Figure S3; Invitrogen), a FANCA-specific Stealth RNA (5′-AAGGGUCAAG AGGGAAAAAUA-3′, for Supplementary Figure S4; Invitrogen), and the control RNA (Negative Control Medium; Invitrogen) were introduced into HeLa cells expressing histone H3-GFP by Lipofectamine2000 (Invitrogen), as described (Kimura *et al*, 2006). Total cellular proteins were prepared 0–4 days after the RNA introduction, separated by 8% SDS–PAGE, and immunoblotted with a mouse monoclonal antibody directed against either FANCD2 (1:250; FI17, Santa Cruz Biotechnology, Inc.), α-tubulin (1:1000; Sigma) as a loading control, or an antibody against FANCA (1:1000; rabbit polyclonal, Bethyl Laboratories, Inc.). Secondary detection was performed with a sheep anti-mouse IgG, horseradish peroxidase-linked species-specific $F(ab')_2$ fragment (GE Healthcare; 1:500 for FANCD2 and 1:1000 for α-tubulin), or a sheep anti-rabbit IgG, horseradish peroxidase-linked species-specific $F(ab')_2$ fragment (GE Healthcare; 1:1000 for FANCA). The signals were detected by chemiluminescence (Western Lightning Plus; Perkin Elmer).

To generate HeLa cells expressing both H3-GFP and mCherry-PCNA, cells expressing H3-GFP (blasticidin resistance; Kimura and Cook, 2001) and mCherry-PCNA (puromycin resistance; generated using pMX-puro-based expression vector carrying mCherry-PCNA; Leonhardt *et al*, 2000; Kitamura *et al*, 2003) were fused using polyethylene glycol (Roche; Kimura and Cook, 2001), and single colonies were selected in the presence of 1 μg/ml blasticidin and 0.5 μg/ml puromycin.

FRAP was performed 3–4 days after siRNA transfection as described (Kimura *et al*, 2006), using a confocal microscope (FV-1000; Olympus) with a × 60 UPlanSApo NA = 1.35 lens. Three confocal images of a field containing 4–10 nuclei were collected (800 × 800 pixels, zoom 3, scan speed 2 μs/pixel, pinhole 800 μm, Kalman filtration for four scans, LP505 emission filter, and 0.1% transmission of 488-nm Ar laser), one half of each nucleus was bleached using 75% transmission of 488 nm and 100% of 514 nm (two iterations), and images were obtained using the original setting at 1 min intervals.

For the complementation experiments, RNAi-resistant *hFANCD2* genes were constructed by introducing silent mutations in the FANCD2-specific Stealth RNA (no. 1) target sequence (5′-TCTGCTAAAGAG-3′) as follows: 5′-TCCGCCAAGGAA-3′. HeLa cells expressing histone H3-GFP were transfected with the FANCD2-specific Stealth RNAs (no. 1) to knockdown the endogenous hFANCD2. The next day, the cells were transfected with the RNAi-resistant mCherry-*hFANCD2*, mCherry-*hFANCD2(R302W)*, or mCherry-*hFANCD2(K561R)* gene, using the FuGENE system (Promega), and were further grown for 2 days before FRAP. After FRAP, the glass-bottom dish was processed for immunofluorescence.

The fluorescence intensity of the bleached area was measured using Image J 1.39u (W Rasband; http://rsb.info.nih.gov/ij/). After subtracting the background, the intensity was normalized to the initial intensity before bleaching.

Immunofluorescence

For immunofluorescence, HeLa cells expressing histone H3-GFP were grown on a glass-bottom dish (Mat-tek), transfected with Stealth RNA, and fixed with 4% paraformaldehyde at 3 days after transfection. The fixed cells were permeabilized and stained using mouse anti-FANCD2 (1:250) and goat Cy3-conjugated anti-mouse IgG (1:500; Jackson Immunoresearch). When mCherry-*hFANCD2* was transfected, goat Cy5-conjugated anti-mouse IgG (1:500; Jackson Immunoresearch) was used as the secondary antibody. For double staining with FANCA, rabbit anti-FANCA (1:100; Bethyl Laboratories, Inc.) and goat Cy5-conjugated anti-rabbit IgG (1:500; Jackson Immunoresearch) are also used. DNA was counterstained with DAPI. The fluorescence images were obtained using a confocal microscope (Olympus FV-1000 with a × 60 UPlanSApo NA = 1.35 oil-immersion objective lens; or Carl Zeiss LSM510 with a × 40 C-Apo NA = 1.2 water-immersion objective lens).

Generation of the FANCD2$^{-/-}$ DT40 cells producing the FANCD2 mutants

Plasmids for the cFANCD2-mutant fusions were constructed in the pcDNA3.1-based GFP or histone H2B-GFP expression vector, by inserting FANCD2 fragments using the Gateway system (Invitrogen). To obtain stably expressing clones, these plasmids were transfected into *FANCD2*-deficient DT40 cells (Yamamoto *et al*, 2005), and the clones expressing the fusions were identified by measuring the GFP fluorescence with a FACSCalibur (Becton Dickinson), as described (Yamamoto *et al*, 2003; Ishiai *et al*, 2004).

Cisplatin sensitivity assay

Sensitivity to cisplatin (Nihon-Kayaku) was assayed by colony formation, in medium containing 1.4% methylcellulose and the indicated dosage of cisplatin (Yamamoto *et al*, 2003; Ishiai *et al*, 2004).

Cell fractionation and detection of FANCD2/FANCI proteins

The indicated cells were either treated with MMC (500 ng/ml for 6 h) or left untreated, and were fractionated into soluble and chromatin fractions, as described previously (Matsushita *et al*, 2005; Ishiai *et al*, 2008). Pull-down assays of cFANCD2-H2B-GFP proteins were performed using anti-GFP beads (MBL). The proteins were separated by 6% SDS–PAGE, and were detected by western blotting. The anti-chicken FANCD2 and FANCI antibodies were obtained by immunizing rabbits with the bacterially expressed His fusion protein with full-length chicken FANCD2 and the GST fusion protein with chicken FANCI (amino acids 1–251), respectively.

Gel filtration analysis

The purified cFANCD2 and cFANCI proteins were analysed by Superdex 200 HR 10/30 (GE Healthcare) gel filtration chromatography. The elution buffer contained 20 mM Tris–HCl (pH 8.0), 200 mM NaCl, 10% glycerol, and 1 mM DTT.

Supplementary data

Supplementary data are available at *The EMBO Journal* Online (http://www.embojournal.org).

Acknowledgements

We would like to thank Emi Uchida for expert technical assistance, and M Cristina Cardoso, Toshio Kitamura, and Shin-ya Isobe for materials. This work was supported in part by Grants-in-Aid from the Japanese Society for the Promotion of Science (JSPS), and the Ministry of Education, Culture, Sports, Science and Technology (MEXT), Japan. H Kurumizaka was also supported by the Waseda Research Institute for Science and Engineering, the Sagawa Foundation for Promotion of Cancer Research, and NOVARTIS

Foundation (Japan) for the Promotion of Science. MI was supported by the Ichiro Kanehara Foundation and the Mochida Memorial Foundation for Medical and Pharmaceutical Research.

Author contributions: KS, KT, SF, YT, AO, HT, and WK purified FANCD2, FANCI, and histones, and KS and KT performed biochemical analyses. MI, H Kitao, and MT performed genetic and cell biological analyses. KS and H Kimura performed FRAP analyses. KS and ND performed domain analysis of FANCD2 by mass spectroscopy. AO, HT, and CO performed proteome analysis of histone-binding proteins. H Kurumizaka and MT conceived, designed, and supervised all of the work, and KS and H Kurumizaka wrote the paper. All of the authors discussed the results and commented on the manuscript.

Conflict of interest

The authors declare that they have no conflict of interest.

References

Ali AM, Pradhan A, Singh TR, Du C, Li J, Wahengbam K, Grassman E, Auerbach AD, Pang Q, Meetei AR (2012) FAAP20: a novel ubiquitin-binding FA nuclear core-complex protein required for functional integrity of the FA-BRCA DNA repair pathway. *Blood* **119:** 3285–3294

Avvakumov N, Nourani A, Côté J (2011) Histone chaperones: modulators of chromatin marks. *Mol Cell* **41:** 502–514

Bhagwat N, Olsen AL, Wang AT, Hanada K, Stuckert P, Kanaar R, D'Andrea A, Niedernhofer LJ, McHugh PJ (2009) XPF-ERCC1 participates in the Fanconi anemia pathway of cross-link repair. *Mol Cell Biol* **29:** 6427–6437

Bradford MM (1976) A rapid and sensitive method for the quantitation of microgram quantities of protein utilizing the principle of protein-dye binding. *Anal Biochem* **72:** 248–254

Crossan GP, van der Weyden L, Rosado IV, Langevin F, Gaillard PH, McIntyre RE; Sanger Mouse Genetics Project, Gallagher F, Kettunen MI, Lewis DY, Brindle K, Arends MJ, Adams DJ, Patel KJ (2011) Disruption of mouse Slx4, a regulator of structure-specific nucleases, phenocopies Fanconi anemia. *Nat Genet* **43:** 147–152

Dunleavy EM, Roche D, Tagami H, Lacoste N, Ray-Gallet D, Nakamura Y, Daigo Y, Nakatani Y, Almouzni G (2009) HJURP is a cell-cycle-dependent maintenance and deposition factor of CENP-A at centromeres. *Cell* **137:** 485–497

English CM, Adkins MW, Carson JJ, Churchill ME, Tyler JK (2006) Structural basis for the histone chaperone activity of Asf1. *Cell* **127:** 495–508

Fekairi S, Scaglione S, Chahwan C, Taylor ER, Tissier A, Coulon S, Dong MQ, Ruse C, Yates 3rd JR, Russell P, Fuchs RP, McGowan CH, Gaillard PH (2009) Human SLX4 is a Holliday junction resolvase subunit that binds multiple DNA repair/recombination endonucleases. *Cell* **138:** 78–89

Foltz DR, Jansen LET, Bailey AO, Yates JR, Bassett EA, Wood S, Black BE, Cleveland DW (2009) Centromere-specific assembly of CENP-A nucleosomes is mediated by HJURP. *Cell* **137:** 472–484

Garcia-Higuera I, Taniguchi T, Ganesan S, Meyn MS, Timmers C, Hejna J, Grompe M, D'Andrea AD (2001) Interaction of the Fanconi anemia proteins and BRCA1 in a common pathway. *Mol Cell* **7:** 249–262

Garner E, Smogorzewska A (2011) Ubiquitylation and the Fanconi anemia pathway. *FEBS Lett* **585:** 2853–2860

Hejna J, Holtorf M, Hines J, Mathewson L, Hemphill A, Al-Dhalimy M, Olson SB, Moses RE (2008) Tip60 is required for DNA interstrand cross-link repair in the Fanconi anemia pathway. *J Biol Chem* **283:** 9844–9851

Hicks JK, Chute CL, Paulsen MT, Ragland RL, Howlett NG, Guéranger Q, Glover TW, Canman CE (2010) Differential roles for DNA polymerases eta, zeta, and REV1 in lesion bypass of intrastrand versus interstrand DNA cross-links. *Mol Cell Biol* **30:** 1217–1230

Hu H, Liu Y, Wang M, Fang J, Huang H, Yang N, Li Y, Wang J, Yao X, Shi Y, Li G, Xu RM (2011) Structure of a CENP-A-histone H4 heterodimer in complex with chaperone HJURP. *Genes Dev* **25:** 901–906

Ishiai M, Kimura M, Namikoshi K, Yamazoe M, Yamamoto K, Arakawa H, Agematsu K, Matsushita N, Takeda S, Buerstedde JM, Takata M (2004) DNA cross-link repair protein SNM1A interacts with PIAS1 in nuclear focus formation. *Mol Cell Biol* **24:** 10733–10741

Ishiai M, Kitao H, Smogorzewska A, Tomida J, Kinomura A, Uchida E, Saberi A, Kinoshita E, Kinoshita-Kikuta E, Koike T, Tashiro S, Elledge SJ, Takata M (2008) FANCI phosphorylation functions as a molecular switch to turn on the Fanconi anemia pathway. *Nat Struct Mol Biol* **15:** 1138–1146

Joo W, Xu G, Persky NS, Smogorzewska A, Rudge DG, Buzovetsky O, Elledge SJ, Pavletich NP (2011) Structure of the FANCI-FANCD2 complex: insights into the Fanconi anemia DNA repair pathway. *Science* **333:** 312–316

Kee Y, D'Andrea AD (2010) Expanded roles of the Fanconi anemia pathway in preserving genomic stability. *Genes Dev* **24:** 1680–16943

Kim H, Yang K, Dejsuphong D, D'Andrea AD (2012) Regulation of Rev1 by the Fanconi anemia core complex. *Nat Struct Mol Biol* **19:** 164–170

Kim Y, Lach FP, Desetty R, Hanenberg H, Auerbach AD, Smogorzewska A (2011) Mutations of the *SLX4* gene in Fanconi anemia. *Nat Genet* **43:** 142–146

Kimura H, Cook PR (2001) Kinetics of core histones in living human cells: little exchange of H3 and H4 and some rapid exchange of H2B. *J Cell Biol* **153:** 1341–1353

Kimura H, Takizawa N, Allemand E, Hori T, Iborra FJ, Nozaki N, Muraki M, Hagiwara M, Krainer AR, Fukagawa T, Okawa K (2006) A novel histone-exchange factor, protein phosphatase 2Cγ, mediates the exchange and dephosphorylation of H2A-H2B. *J Cell Biol* **175:** 389–400

Kitamura T, Koshino Y, Shibata F, Oki T, Nakajima H, Nosaka T, Kumagai H (2003) Retrovirus-mediated gene transfer and expression cloning: powerful tools in functional genomics. *Exp Hematol* **31:** 1007–1014

Kitao H, Takata M (2011) Fanconi anemia: a disorder defective in the DNA damage response. *Int J Hematol* **93:** 417–424

Knipscheer P, Räschle M, Smogorzewska A, Enoiu M, Ho TV, Schärer OD, Elledge SJ, Walter JC (2009) The Fanconi anemia pathway promotes replication-dependent DNA interstrand cross-link repair. *Science* **326:** 1698–1701

Kratz K, Schöpf B, Kaden S, Sendoel A, Eberhard R, Lademann C, Cannavó E, Sartori AA, Hengartner MO, Jiricny J (2010) Deficiency of FANCD2-associated nuclease KIAA1018/FAN1 sensitizes cells to interstrand crosslinking agents. *Cell* **142:** 77–88

Leonhardt H, Rahn HP, Weinzierl P, Sporbert A, Cremer T, Zink D, Cardoso MC (2000) Dynamics of DNA replication factories in living cells. *J Cell Biol* **149:** 271–280

Leung JW, Wang Y, Fong KW, Huen MS, Li L, Chen J (2012) Fanconi anemia (FA) binding protein FAAP20 stabilizes FA complementation group A (FANCA) and participates in interstrand cross-link repair. *Proc Natl Acad Sci USA* **109:** 4491–4496

MacKay C, Déclais AC, Lundin C, Agostinho A, Deans AJ, MacArtney TJ, Hofmann K, Gartner A, West SC, Helleday T, Lilley DM, Rouse J (2010) Identification of KIAA1018/FAN1, a DNA repair nuclease recruited to DNA damage by monoubiquitinated FANCD2. *Cell* **142:** 65–76

Matsushita N, Kitao H, Ishiai M, Nagashima N, Hirano S, Okawa K, Ohta T, Yu DS, McHugh PJ, Hickson ID, Venkitaraman AR, Kurumizaka H, Takata M (2005) A FancD2-monoubiquitin fusion reveals hidden functions of Fanconi anemia core complex in DNA repair. *Mol Cell* **19:** 841–847

Meetei AR, de Winter JP, Medhurst AL, Wallisch M, Waisfisz Q, van de Vrugt HJ, Oostra AB, Yan Z, Ling C, Bishop CE, Hoatlin ME, Joenje H, Wang W (2003) A novel ubiquitin ligase is deficient in Fanconi anemia. *Nat Genet* **35:** 165–170

Natsume R, Eitoku M, Akai Y, Sano N, Horikoshi M, Senda T (2007) Structure and function of the histone chaperone CIA/ASF1 complexed with histones H3 and H4. *Nature* **446:** 338–341

Niedernhofer LJ, Lalai AS, Hoeijmakers JHJ (2005) Fanconi anemia (cross)linked to DNA repair. *Cell* **123:** 1191–1198

Nomura Y, Adachi N, Koyama H (2007) Human Mus81 and FANCB independently contribute to repair of DNA damage during replication. *Genes Cells* **12:** 1111–1122

Nozawa RS, Nagao K, Masuda HT, Iwasaki O, Hirota T, Nozaki N, Kimura H, Obuse C (2010) Human POGZ modulates dissociation of HP1alpha from mitotic chromosome arms through Aurora B activation. *Nat Cell Biol* **12:** 719–727

Osakabe A, Tachiwana H, Matsunaga T, Shiga T, Nozawa RS, Obuse C, Kurumizaka H (2010) Nucleosome formation activity of human somatic nuclear autoantigenic sperm protein (sNASP). *J Biol Chem* **285:** 11913–11921

Pace P, Mosedale G, Hodskinson MR, Rosado IV, Sivasubramaniam M & Patel KJ (2010) Ku70 corrupts DNA repair in the absence of the Fanconi anemia pathway. *Science* **329:** 219–223

Sato K, Toda K, Ishiai M, Takata M, Kurumizaka H (2012) DNA robustly stimulates FANCD2 monoubiquitylation in the complex with FANCI. *Nucleic Acids Res* **40:** 4553–4561

Seki S, Ohzeki M, Uchida A, Hirano S, Matsushita N, Kitao H, Oda T, Yamashita T, Kashihara N, Tsubahara A, Takata M, Ishiai M (2007) A requirement of FancL and FancD2 monoubiquitination in DNA repair. *Genes Cells* **12:** 299–310

Sims AE, Spiteri E, Sims 3rd RJ, Arita AG, Lach FP, Landers T, Wurm M, Freund M, Neveling K, Hanenberg H, Auerbach AD, Huang TT (2007) FANCI is a second monoubiquitinated member of the Fanconi anemia pathway. *Nat Struct Mol Biol* **14:** 564–567

Smogorzewska A, Desetty R, Saito TT, Schlabach M, Lach FP, Sowa ME, Clark AB, Kunkel TA, Harper JW, Colaiácovo MP, Elledge SJ (2010) A genetic screen identifies FAN1, a Fanconi anemia-associated nuclease necessary for DNA interstrand crosslink repair. *Mol Cell* **39:** 36–47

Smogorzewska A, Matsuoka S, Vinciguerra P, McDonald 3rd ER, Hurov KE, Luo J, Ballif BA, Gygi SP, Hofmann K, D'Andrea AD, Elledge SJ (2007) Identification of the FANCI protein, a monoubiquitinated FANCD2 paralog required for DNA repair. *Cell* **129:** 289–301

Stoepker C, Hain K, Schuster B, Hilhorst-Hofstee Y, Rooimans MA, Steltenpool J, Oostra AB, Eirich K, Korthof ET, Nieuwint AW, Jaspers NG, Bettecken T, Joenje H, Schindler D, Rouse J, de Winter JP (2011) SLX4, a coordinator of structure-specific endonucleases, is mutated in a new Fanconi anemia subtype. *Nat Genet* **43:** 138–141

Svendsen JM, Smogorzewska A, Sowa ME, O'Connell BC, Gygi SP, Elledge SJ, Harper JW (2009) Mammalian BTBD12/SLX4 assembles a Holliday junction resolvase and is required for DNA repair. *Cell* **138:** 63–77

Tachiwana H, Kagawa W, Osakabe A, Kawaguchi K, Shiga T, Hayashi-Takanaka Y, Kimura H, Kurumizaka H (2010) Structural basis of instability of the nucleosome containing a testis-specific histone variant, human H3T. *Proc Natl Acad Sci USA* **107:** 10454–10459

Tachiwana H, Kagawa W, Shiga T, Osakabe A, Miya Y, Saito K, Hayashi-Takanaka Y, Oda T, Sato M, Park S-Y, Kimura H, Kurumizaka H (2011a) Crystal structure of the human centromeric nucleosome containing CENP-A. *Nature* **476:** 232–235

Tachiwana H, Osakabe A, Kimura H, Kurumizaka H (2008) Nucleosome formation with the testis-specific histone H3 variant, H3t, by human nucleosome assembly proteins in vitro. *Nucleic Acids Res* **36:** 2208–2218

Tachiwana H, Osakabe A, Shiga T, Miya Y, Kimura H, Kagawa W, Kurumizaka H (2011b) Structures of human nucleosomes containing major histone H3 variants. *Acta Cryst D* **67**(Pt 6): 578–583

Tanaka Y, Tawaramoto-Sasanuma M, Kawaguchi S, Ohta T, Yoda K, Kurumizaka H, Yokoyama S (2004) Expression and purification of recombinant human histones. *Methods* **33:** 3–11

Taniguchi T, D'Andrea AD (2006) Molecular pathogenesis of Fanconi anemia: recent progress. *Blood* **107:** 4223–4233

Thompson LH, Hinz JM, Yamada NA, Jones NJ (2005) How Fanconi anemia proteins promote the four Rs: replication, recombination, repair, and recovery. *Environ Mol Mutagen* **45:** 128–142

Timmers C, Taniguchi T, Hejna J, Reifsteck C, Lucas L, Bruun D, Thayer M, Cox B, Olson S, D'Andrea AD, Moses R, Grompe M (2001) Positional cloning of a novel Fanconi anemia gene, *FANCD2*. *Mol Cell* **7:** 241–248

Vaz F, Hanenberg H, Schuster B, Barker K, Wiek C, Erven V, Neveling K, Endt D, Kesterton I, Autore F, Fraternali F, Freund M, Hartmann L, Grimwade D, Roberts RG, Schaal H, Mohammed S, Rahman N, Schindler D, Mathew CG (2010) Mutation of the *RAD51C* gene in a Fanconi anemia-like disorder. *Nat Genet* **42:** 406–409

Venkitaraman AR (2004) Tracing the network connecting BRCA and Fanconi anaemia proteins. *Nat Rev Cancer* **4:** 435–445

Wang W (2007) Emergence of a DNA-damage response network consisting of Fanconi anaemia and BRCA proteins. *Nat Rev Genet* **8:** 735–748

Wolffe A (1998) *Chromatin: Structure and Function*. 3rd ednSan Diego, California, USA: Academic Press

Yamamoto K, Hirano S, Ishiai M, Morishima K, Kitao H, Namikoshi K, Kimura M, Matsushita N, Arakawa H, Buerstedde JM, Komatsu K, Thompson LH, Takata M (2005) Fanconi anemia protein FANCD2 promotes immunoglobulin gene conversion and DNA repair through a mechanism related to homologous recombination. *Mol Cell Biol* **25:** 34–43

Yamamoto K, Ishiai M, Matsushita N, Arakawa H, Lamerdin JE, Buerstedde JM, Tanimoto M, Harada M, Thompson LH, Takata M (2003) Fanconi anemia FANCG protein in mitigating radiation- and enzyme-induced DNA double-strand breaks by homologous recombination in vertebrate cells. *Mol Cell Biol* **23:** 5421–5430

Yamamoto KN, Kobayashi S, Tsuda M, Kurumizaka H, Takata M, Kono K, Jiricny J, Takeda S, Hirota K (2011) Involvement of SLX4 in interstrand cross-link repair is regulated by the Fanconi anemia pathway. *Proc Natl Acad Sci USA* **108:** 6492–6496

Yoshikiyo K, Kratz K, Hirota K, Nishihara K, Takata M, Kurumizaka H, Horimoto S, Takeda S, Jiricny J (2010) KIAA1018/FAN1 nuclease protects cells against genomic instability induced by interstrand cross-linking agents. *Proc Natl Acad Sci USA* **107:** 21553–21557

Please cite this article in press as: Nishimura et al., Mcm8 and Mcm9 Form a Complex that Functions in Homologous Recombination Repair Induced by DNA Interstrand Crosslinks, Molecular Cell (2012), http://dx.doi.org/10.1016/j.molcel.2012.05.047

Molecular Cell
Article

Mcm8 and Mcm9 Form a Complex that Functions in Homologous Recombination Repair Induced by DNA Interstrand Crosslinks

Kohei Nishimura,[1] Masamichi Ishiai,[2] Kazuki Horikawa,[1,3] Tatsuo Fukagawa,[3,4] Minoru Takata,[2] Haruhiko Takisawa,[5] and Masato T. Kanemaki[1,3,*]
[1]Center for Frontier Research, National Institute of Genetics, Research Organization of Information and Systems, Yata 1111, Mishima, Shizuoka 411-8540, Japan
[2]Department of Late Effects Studies, Radiation Biology Center, Kyoto University, Yoshidakonoe-cho, Sakyo-ku, Kyoto 606-8501, Japan
[3]Department of Genetics, SOKENDAI, Yata 1111, Mishima, Shizuoka 411-8540, Japan
[4]Division of Molecular Genetics, National Institute of Genetics, Yata 1111, Mishima, Shizuoka 411-8540
[5]Department of Biological Sciences, Graduate School of Science, Osaka University, Machikaneyama 1-1, Toyonaka, Osaka 560-0043, Japan
*Correspondence: mkanemak@nig.ac.jp
http://dx.doi.org/10.1016/j.molcel.2012.05.047

SUMMARY

DNA interstrand crosslinks (ICLs) are highly toxic lesions that stall the replication fork to initiate the repair process during the S phase of vertebrates. Proteins involved in Fanconi anemia (FA), nucleotide excision repair (NER), and translesion synthesis (TS) collaboratively lead to homologous recombination (HR) repair. However, it is not understood how ICL-induced HR repair is carried out and completed. Here, we showed that the replicative helicase-related Mcm family of proteins, Mcm8 and Mcm9, forms a complex required for HR repair induced by ICLs. Chicken DT40 cells lacking *MCM8* or *MCM9* are viable but highly sensitive to ICL-inducing agents, and exhibit more chromosome aberrations in the presence of mitomycin C compared with wild-type cells. During ICL repair, Mcm8 and Mcm9 form nuclear foci that partly colocalize with Rad51. Mcm8-9 works downstream of the FA and BRCA2/Rad51 pathways, and is required for HR that promotes sister chromatid exchanges, probably as a hexameric ATPase/helicase.

INTRODUCTION

DNA interstrand crosslinks (ICLs) are covalent links between the double helix that are highly toxic to cells because this type of DNA damage impedes DNA unwinding during DNA replication and transcription. Based on this toxicity, especially in proliferating cells, ICL-inducing agents (such as mitomycin C [MMC] and cisplatin) have been used widely as cancer chemotherapeutic agents (Deans and West, 2011). Therefore, it is important to understand how ICLs are recognized, processed, and repaired in cells. Compared with other types of DNA damage, ICLs are unique because they are mainly repaired during the S phase in vertebrates (Akkari et al., 2000). ICLs are repaired through a coordination of proteins involved in nucleotide excision repair (NER), translesion synthesis (TLS), and homologous recombination (HR). The 15 Fanconi anemia (FA) proteins, which are involved in the genetic disorder FA, orchestrate these repair proteins (Kee and D'Andrea, 2010; Moldovan and D'Andrea, 2009).

ICL repair is initiated by the encounter of replication fork to ICLs. After the stalling of the fork, the FA core ubiquitin ligase complex, which comprises eight FA (A, B, C, E, F, G, L, and M) and other proteins, is activated to monoubiquitylate the FANCI-FANCD2 (ID) complex (Garcia-Higuera et al., 2001; Moldovan and D'Andrea, 2009). It is thought that this ubiquitylation promotes chromatin association of the ID complex for the recruitment of ubiquitin-interacting factors, such as FAN1 and SLX4 (Kee and D'Andrea, 2010; Yamamoto et al., 2011). At least three nuclease complexes, Mus81-Eme1, XPF-ERCC1, and FAN1, are involved in the subsequent process, which leads to the generation of a double-strand break (DSB) and incision of the crosslinked bases (Hanada et al., 2006; Niedernhofer et al., 2004). Then, the TLS polymerases, REV1 and Pol ζ (a complex composed of REV3 and REV7), synthesize DNA over the site of the crosslink (Niedzwiedz et al., 2004; Raschle et al., 2008; Simpson and Sale, 2003; Sonoda et al., 2003). Under the control of BRCA2 (also called FANCD1), Rad51 is loaded onto the site of damage independently of the FA pathway and participates in the subsequent HR repair (Godthelp et al., 2002; Kitao et al., 2006; Long et al., 2011). Even though Rad51 and the five Rad51 paralogs are involved in this process (Liu et al., 1998; Takata et al., 2000; Takata et al., 2001), it is unclear how the repair is carried out and completed downstream of Rad51 (Deans and West, 2011).

The hexameric Mcm2-7 complex is the replicative helicase that unwinds dsDNA at the replication fork (Bochman and Schwacha, 2009) and stalls in front of ICLs during replication elongation (Raschle et al., 2008). All six evolutionarily related subunits belong to the AAA+ superfamily (Hanson and Whiteheart, 2005) and contain the Mcm family domain, which

Please cite this article in press as: Nishimura et al., Mcm8 and Mcm9 Form a Complex that Functions in Homologous Recombination Repair Induced by DNA Interstrand Crosslinks, Molecular Cell (2012), http://dx.doi.org/10.1016/j.molcel.2012.05.047

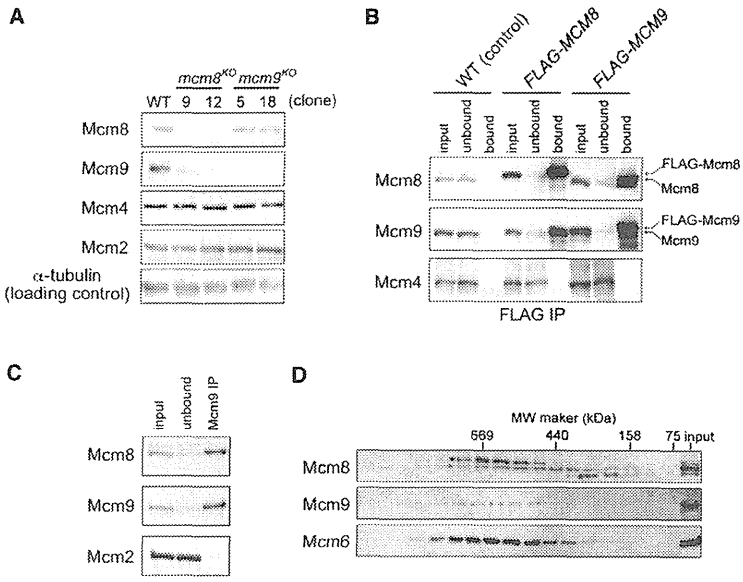

Figure 1. Mcm8 and Mcm9 Form a Complex that Is Distinct from Mcm2-7

(A) Expression of proteins in *mcm8*^{KO} and *mcm9*^{KO} cells. Extracts prepared from *mcm8*^{KO} and *mcm9*^{KO} clones were processed to detect the indicated proteins using immunoblotting.

(B) Mcm8 and Mcm9 form a complex. FLAG immunoprecipitants from extracts of cells expressing FLAG-Mcm8 or FLAG-Mcm9 were blotted using anti-Mcm8, anti-Mcm9 and anti-Mcm4 antibodies.

(C) Endogenous Mcm8 and Mcm9 exist mostly as a complex. Anti-Mcm9 immunoprecipitants from wild-type extracts were blotted using anti-Mcm8, anti-Mcm9, and anti-Mcm2 antibodies.

(D) Molecular size of the Mcm8-9 complex. Whole-cell extracts prepared from wild-type cells were fractionated using a Superose 6 gel filtration column. Fractions were processed to detect Mcm8 and Mcm6 by immunoblotting. Asterisks indicate background proteins.

includes motifs that are required for ATP hydrolysis (such as the Walker A and B, and R-finger motifs). A subset of eukaryotes expresses two additional proteins of the Mcm family, namely Mcm8 and Mcm9 (Gozuacik et al., 2003; Johnson et al., 2003; Lutzmann et al., 2005; Yoshida, 2005). In *Xenopus*, Mcm8 and Mcm9 are required for fork elongation and Mcm2-7 loading, respectively (Lutzmann and Mechali, 2008; Maiorano et al., 2005). In humans, Mcm8 is reportedly required for the assembly of the prereplicative complex during the G1 phase (Volkening and Hoffmann, 2005). Very recently, knockout mice of the *MCM9* gene were successfully generated, indicating that Mcm9 is not essential for DNA replication (Hartford et al., 2011). *Drosophila* is the only organism that has *MCM8* (also called *REC*) without *MCM9*, and genetic analyses revealed that *Drosophila* Mcm8/REC is involved in meiotic recombination (Blanton et al., 2005; Matsubayashi and Yamamoto, 2003). In contrast to Mcm2-7, which functions as the replicative helicase from yeast to humans, the reported roles of Mcm8 and Mcm9 are not concordant among species. Intriguingly, a recent phylogenetic analysis suggested that Mcm8 and Mcm9 have a related function (Liu et al., 2009). However, there is no report describing functional characterization of Mcm8 and Mcm9 together.

To address the functional role of Mcm8 and Mcm9 of vertebrate cells, we use genetic analysis with chicken DT40 cells. We demonstrate that Mcm8 and Mcm9 form a complex that is distinct from Mcm2-7. DT40 cells with disruption of the *MCM8* or *MCM9* gene reveal that the encoding proteins are not essential for cell viability, showing that both proteins do not play an essential role in DNA replication. *MCM8* or *MCM9* knockout cells exhibit similar defects regarding normal growth and hypersensitivity to ICL-inducing agents, but not to IR. Mcm8 and Mcm9 play a role downstream of the FA and BRCA2/Rad51 pathways, possibly as a hexameric ATPase/DNA helicase, and are involved in HR and sister chromatid exchanges (SCEs). We conclude that the Mcm8-9 complex is required in ICL-induced HR repair. Our results also imply that Mcm8-9 is involved in a distinctive HR system important for ICL repair in vertebrate cells.

RESULTS

Mcm8 and Mcm9 Are Not Essential for Cell Viability

To characterize the function of Mcm8 and Mcm9, we used chicken DT40 cells, as the genomic DNA of these cells can be modified using HR-mediated targeting (Buerstedde and Takeda, 1991). Initially, we tried to disrupt the *MCM8* or *MCM9* gene to determine whether these genes are essential for cell viability. To disrupt *MCM8*, we inserted selection markers that deleted exons 6 and 7, which correspond to the upstream region of the Zn-finger motif located at the N terminus of the Mcm8 protein (see Figures S1A and S1B available online). The two *MCM8* alleles were targeted (Figure S1C). The *ASF1* gene is located between exons 6 and 7 of *MCM9*, as is the case for the mouse *MCM9* gene (Figure S1E) (Hartford et al., 2011). In addition to the full length of Mcm9, a shorter isoform that terminates at the alternative exon 7 is expressed in mouse and humans (Blanton et al., 2005; Lutzmann et al., 2005; Yoshida, 2005). Therefore, we inserted selection markers that deleted exon 2, which corresponds to the N-terminal region of Mcm9 containing the Zn-finger motif (Figures S1D and S1E). This insertion destroyed the transcripts of both the full-length protein and the shorter isoform, even if the shorter isoform is also expressed in DT40 cells. Three *MCM9* alleles exist in DT40 cells, all of which were targeted without affecting the expression of *ASF1* mRNA (Figures S1F and S1G). We have successfully generated *MCM8* or *MCM9* knockout cell lines (referred to as *mcm8*^{KO} or *mcm9*^{KO}, respectively). We confirmed that the corresponding proteins were not expressed (Figure 1A), indicating that Mcm8 and Mcm9 are not essential for cell viability. Our results are consistent with the finding of

the study, which demonstrated that *MCM9* is dispensable in mice (Hartford et al., 2011).

Mcm8 and Mcm9 Form a Complex

Interestingly, we found that the expression level of Mcm9 was reduced in $mcm8^{KO}$ cells, even though the expression of Mcm2 and Mcm4, the components of Mcm2-7, were not affected (Figure 1A, $mcm8^{KO}$). The protein levels of Mcm8 in $mcm9^{KO}$ cells were also slightly reduced (Figure 1A, $mcm9^{KO}$). These results suggest that Mcm8 and Mcm9 are unstable in the absence of Mcm9 or Mcm8, respectively. As is often the case with components of a complex, components are destabilized when the complex formation is compromised (e.g., Mcm2-7) (Kawabata et al., 2011). The data described above imply that Mcm8 and Mcm9 may form a complex. Therefore, we investigated whether Mcm8 and Mcm9 form a complex. We generated DT40 cells stably expressing FLAG-tagged Mcm8 or Mcm9 (FLAG-Mcm8 or FLAG-Mcm9) in the $mcm8^{KO}$ or $mcm9^{KO}$ background, respectively. FLAG-Mcm8 and FLAG-Mcm9 were functional in these cells (see below, Figure 2B). FLAG-Mcm8 or FLAG-Mcm9 was immunoprecipitated from cell extracts using an anti-FLAG antibody. We detected Mcm9 in FLAG-Mcm8 immunoprecipitants, and vice versa (Figure 1B). Mcm4 was not detected in the two cases, suggesting that Mcm8 and Mcm9 do not interact with Mcm2-7, as shown previously (Gozuacik et al., 2003; Lutzmann and Mechali, 2008; Maiorano et al., 2005). Importantly, Mcm9 was mostly depleted with FLAG-Mcm8, and vice versa (Figure 1B, see unbound fractions), suggesting that most of Mcm8 and Mcm9 form a complex in these cells. We subjected FLAG-Mcm9 immunoprecipitants to a mass spectrometry analysis and detected Mcm8 but no Mcm2-7 proteins (data not shown). To confirm the formation of a complex between the endogenous Mcm8 and Mcm9 proteins, Mcm9 was immunoprecipitated from extracts of wild-type cells using an anti-Mcm9 antibody. Mcm8 was coprecipitated with Mcm9 (Figure 1C). Furthermore, both Mcm8 and Mcm9 were depleted from the unbound fraction, indicating that the endogenous proteins exist mostly as a complex. Taken together, these results led us to conclude that Mcm8 and Mcm9 form a complex that is distinct from the Mcm2-7 complex.

To determine the molecular size of the Mcm8-9 complex, we fractionated DT40 extracts using a size-exclusion column. We found that Mcm8 and Mcm9 were eluted around the 600 kD fractions, which is similar to the molecular size of the Mcm2-7 complex (Figure 1D) (Davey et al., 2003). In $mcm9^{KO}$ cells, Mcm8 was fractionated between 158 and 440 kD, showing that Mcm8 cannot make a large complex without Mcm9 (Figure S2A). Taking into account the fact that the molecular weights of Mcm8 and Mcm9 are 93 and 130 kDa, respectively, and that many AAA+ superfamily proteins, including Mcm2-7, form a hexamer (Bochman and Schwacha, 2009; Hanson and Whiteheart, 2005), these results suggest that Mcm8 and Mcm9 form a hexameric complex.

Cells Deficient in Mcm8 or Mcm9 Show Similar Growth Defects

Although $mcm8^{KO}$ and $mcm9^{KO}$ cells were viable, they grew slightly slower compared with wild-type cells (Figure S2B). To determine whether the loss of Mcm8 or Mcm9 affected the cell cycle, we analyzed the cells using flow cytometry after BrdU labeling (Figure 2A). The S population was reduced and the G2-M population was increased similarly in $mcm8^{KO}$ and $mcm9^{KO}$ cells. The population of cells containing a lower DNA content was increased in the culture of $mcm8^{KO}$ and $mcm9^{KO}$ cells (Figure 2A, arrowed boxes), indicating that some of these cells die spontaneously. These findings of similar defects in $mcm8^{KO}$ and $mcm9^{KO}$ cells regarding normal growth raise the hypothesis that Mcm8 and Mcm9 play an unidentified role as a complex.

Mcm8 and Mcm9 Are Required for Resistance to ICLs

A possible explanation for the growth defects described above is that cells lacking Mcm8 or Mcm9 have a defect in the repair of DNA damage that occurs naturally. To test this possibility, we studied DNA damage sensitivity in $mcm8^{KO}$ and $mcm9^{KO}$ cells using colony survival assays. We initially tested sensitivity to IR, UV, and MMS (Figure 2B, upper panels). We also tested the $rad18^{KO}$ cells as a control showing mild and high sensitivity to IR and UV, respectively (Yamashita et al., 2002). $mcm8^{KO}$ cells exhibited elevated sensitivity to IR, UV, and MMS, although their IR and UV sensitivities were not as high as those of $rad18^{KO}$. $mcm9^{KO}$ cells were slightly sensitive to UV and MMS, but not to IR. We also tested sensitivity to replication inhibitors, hydroxylurea (HU), and aphidicolin (Figure S2C). We found that $mcm8^{KO}$ and $mcm9^{KO}$ cells are not sensitive to these agents.

Interestingly, we found that both $mcm8^{KO}$ and $mcm9^{KO}$ cells were hypersensitive to the DNA crosslinker cisplatin and MMC (Figure 2B, lower panels). Importantly, the sensitivity to cisplatin and MMC of $mcm8^{KO}$ or $mcm9^{KO}$ cells was suppressed by introducing *FLAG-MCM8* or *FLAG-MCM9*, respectively, indicating that the sensitivity was caused by the loss of Mcm8 or Mcm9. Thus, we concluded that Mcm8 and Mcm9 are required for resistance to DNA crosslinking agents. Taking into the fact that cells deficient in FANCD2 exhibited a similar sensitivity to MMC and cisplatin (Figure 2B, $fancd2^{KO}$), these results suggest the intriguing possibility that the Mcm8-9 complex is involved in ICL repair.

The loss of proteins involved in ICL repair causes chromosome aberrations in the presence of MMC (Moldovan and D'Andrea, 2009; Sasaki and Tonomura, 1973). To study whether the same is true for $mcm8^{KO}$ or $mcm9^{KO}$ cells, we cultured these cells in the presence of MMC for 6 hr and analyzed their mitotic chromosomes. We found a three times increase of chromosome aberrations in $mcm8^{KO}$ or $mcm9^{KO}$ compared with wild-type cells (Figure 2C and Figure S2D), which suggests that Mcm8 and Mcm9 are required for the maintenance of chromosome integrity in the presence of MMC. Subsequently, we established cell lines expressing GFP-Mcm8 or GFP-Mcm9 in the $mcm8^{KO}$ or $mcm9^{KO}$ background, respectively. GFP-Mcm8 and GFP-Mcm9 were functional (see below, Figures 4B and 4C). In the absence of MMC, GFP-Mcm8 and GFP-Mcm9 were detected mainly in the nucleus, but no foci were observed (Figure 3A, −MMC). Conversely, discrete GFP-Mcm8 and GFP-Mcm9 foci were observed in nuclei in the presence of MMC (Figure 3A, +MMC). Moreover, the MMC-induced Mcm8 and Mcm9 foci are colocalized (Figure S2E), suggesting that the

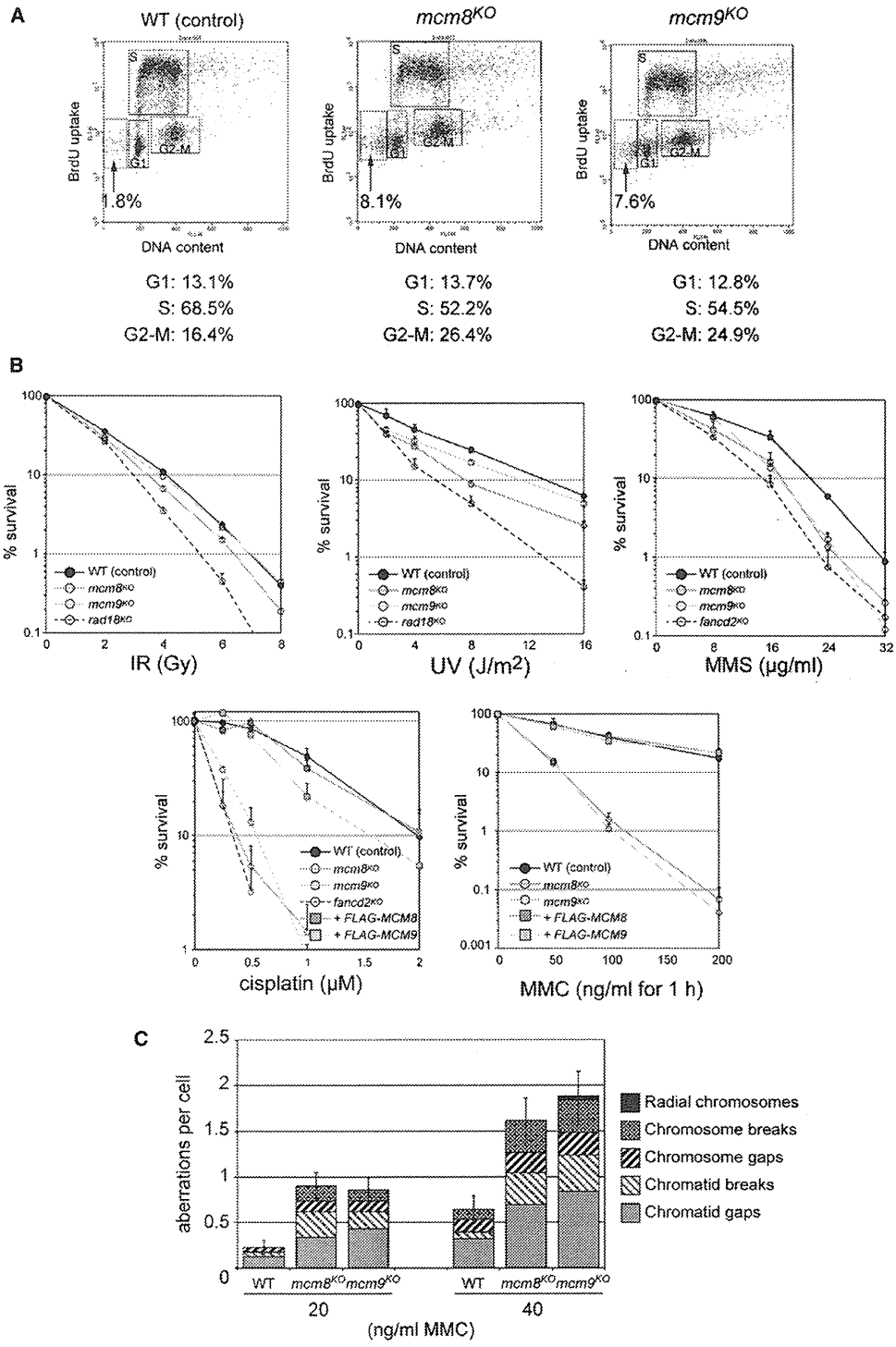

Figure 2. The *mcm8*^{KO} and *mcm9*^{KO} Cells Are Defective in ICL Repair

(A) Cell-cycle profile of the *mcm8*^{KO} and *mcm9*^{KO} cells. Indicated cells were grown and labeled with BrdU for 20 min before being processed using flow cytometry. Arrows indicate dying cells containing a DNA quantity <2C.

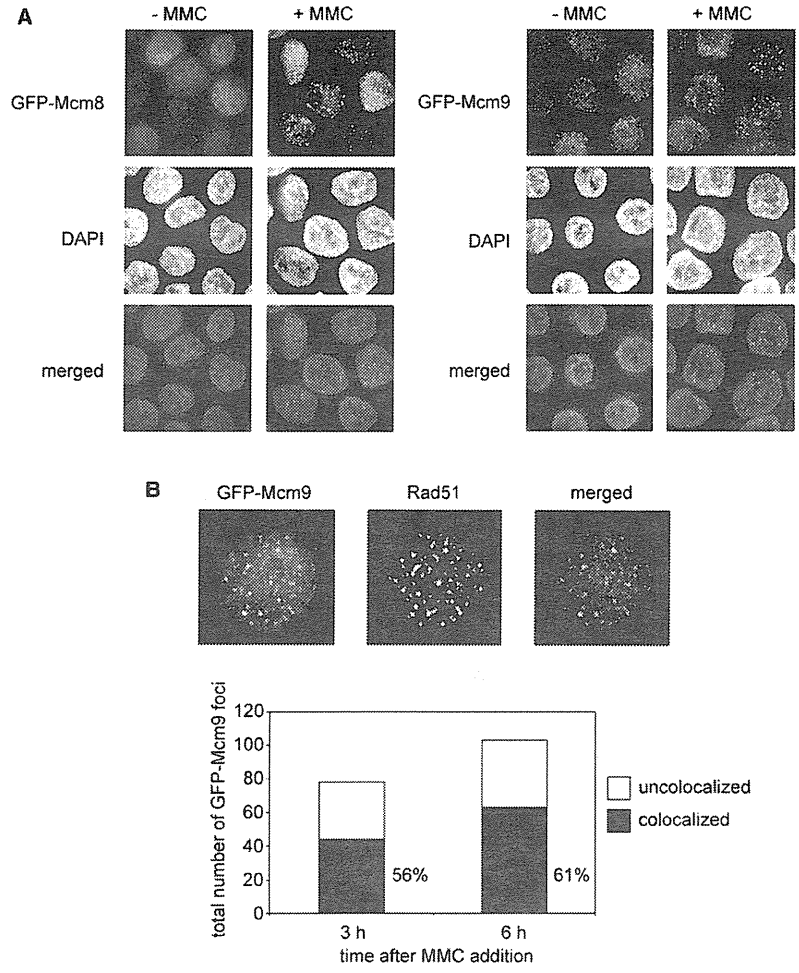

Figure 3. Mcm8 and Mcm9 Make Damage-Dependent Nuclear Foci

(A) MMC-dependent Mcm8 and Mcm9 focus formation. Cells expressing GFP-Mcm8 or GFP-Mcm9 in the *mcm8*^{KO} or *mcm9*^{KO} background, respectively, were grown in the absence or presence of 500 ng/ml of MMC for 6 hr. Fixed cells were stained with DAPI and were analyzed under a fluorescent microscope.

(B) Colocalization of GFP-Mcm9 and Rad51. Cells expressing GFP-Mcm9 in the *mcm9*^{KO} background were cultured as in (A) (pictures). Colocalization of GFP-Mcm9 foci with Rad51 foci in 16 nuclei was quantified at 3 and 6 hr (bar graph).

Mcm8-9 complex associates with damaged DNA or DNA that is being repaired. In fact, more than half of GFP-Mcm9 foci colocalized with Rad51 foci (Figure 3B), suggesting that the Mcm8-9 complex and Rad51 might work in the same repair pathway. Taken together, these results are consistent with the hypothesis that the Mcm8-9 complex is involved in ICL repair.

The Mcm8-9 Complex Participates in ICL Repair, Probably as a Hexameric ATPase/Helicase

All Mcm family proteins have the conserved motifs, Walker A and B, and R finger, which are required for both ATP hydrolysis and helicase activity (Bochman and Schwacha, 2008; Davey et al., 2003; Ilves et al., 2010; Schwacha and Bell, 2001). Therefore, we prepared constructs for the expression of GFP-Mcm8 or GFP-Mcm9 containing an alanine substitution in the Walker A or R-finger motif (Figure 4A). These mutant proteins were stably expressed in *mcm8*^{KO} or *mcm9*^{KO} cells to investigate whether they confer resistance to cisplatin. We confirmed that the expression levels of all mutants were similar (Figures S3A and S3B). Intriguingly, the protein level of endogenous Mcm9 was restored by the expression of GFP-Mcm8 (WT, K452A, or R578A) (Figure S3A), suggesting that GFP-Mcm8 (WT, K452A, and R578A) forms a complex with Mcm9. GFP-Mcm8 (WT) and GFP-Mcm9 (WT) completely suppressed cisplatin sensitivity, indicating that these proteins are functional (Figures 4B and 4C). In sharp contrast, GFP-Mcm8 (K452A and R578A) conferred only minor suppression (Figure 4B), and GFP-Mcm9 (K360A and R484A) did not suppress cisplatin sensitivity at all (Figure 4C). Taking into account the facts that the R-finger motif works in *trans* regarding the ATP hydrolysis of the neighboring ATPase subunit (Bochman et al., 2008; Davey et al., 2003), that many AAA+ proteins form a hexamer (Hanson and Whiteheart, 2005), and that Mcm2-7 works as a hexameric helicase (Bochman and Schwacha, 2008; Ilves et al., 2010), these results suggest that Mcm8 and Mcm9 work as a hexameric ATPase/helicase complex. We concluded that the ATPase activity of both Mcm8 and Mcm9 is essential for the role of the Mcm8-9 complex in cisplatin resistance.

We tested the formation of foci of the GFP-Mcm8 mutants after MMC treatment. K452A mutant cells were defective in the formation of foci, whereas R578A cells formed much fewer and faint foci (Figure 4D). Similar results were obtained for the

(B) Sensitivity to DNA damage in *mcm8*^{KO} and *mcm9*^{KO} cells. Indicated cells were analyzed using a colony-formation assay. Mean ± SD of three independent experiments is shown.

(C) Levels of chromosome aberrations in wild-type, *mcm8*^{KO}, and *mcm9*^{KO} cells after treatment of 20 or 40 ng/ml of MMC for 24 hr. Observed chromosome aberrations were also indicated. At least 50 mitotic nuclei were analyzed. Error bars indicate SD of total aberrations per metaphase.

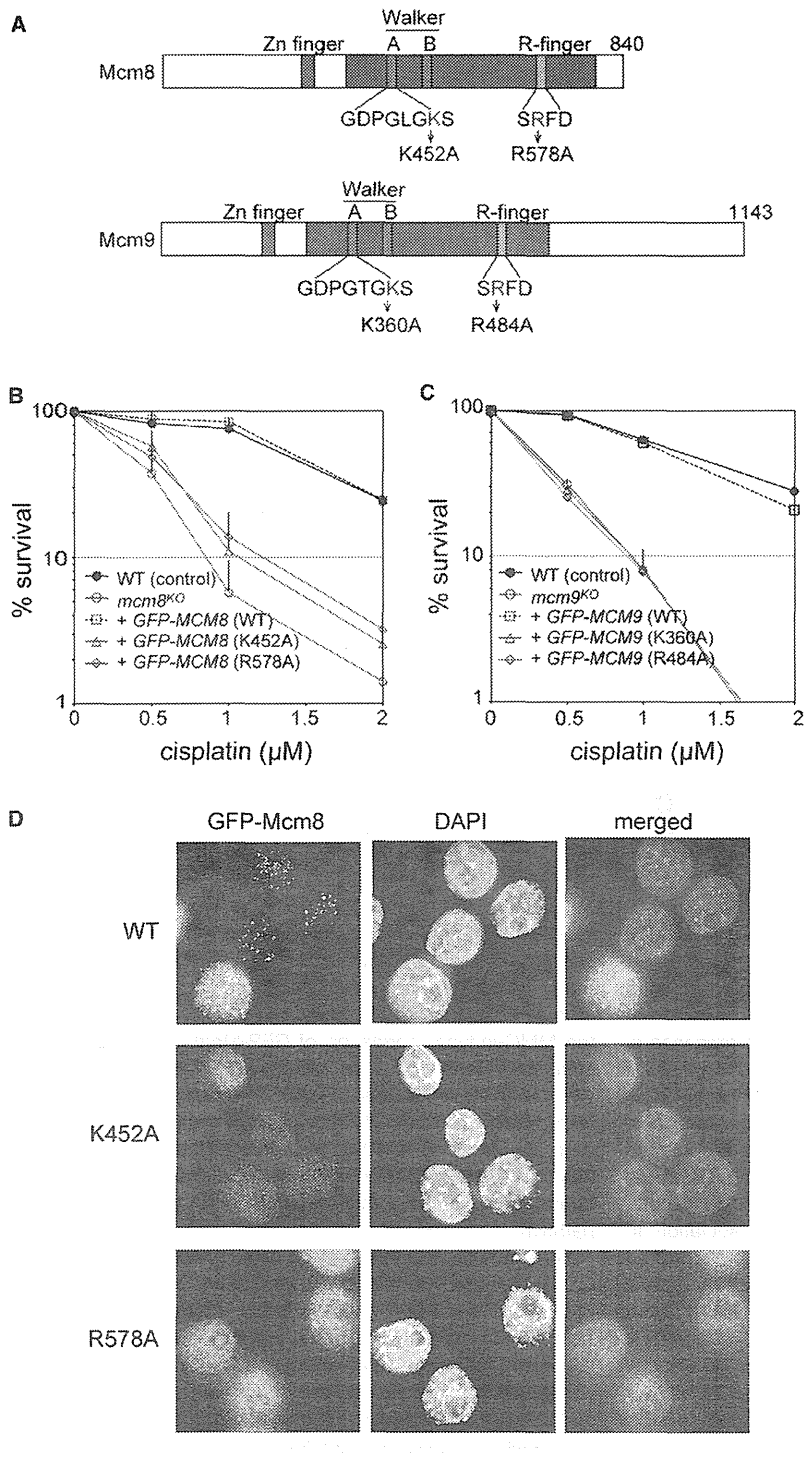

Figure 4. Mcm8 and Mcm9 Are Required for ICL Resistance, Possibly as an ATPase/Helicase Complex

(A) Schematic illustration of the domain architecture of chicken Mcm8 and Mcm9. Mutations introduced into the Walker A and R-finger motifs are indicated.

(B and C) Sensitivity to cisplatin in cells expressing Mcm8 or Mcm9 mutants. Cells expressing the indicated mutants of GFP-Mcm8 or GFP-Mcm9 in the *mcm8*^{KO} or *mcm9*^{KO} background were analyzed using a colony-formation assay. Mean ± SD of three independent experiments is shown.

(D) MMC-induced foci formation of GFP-Mcm8 mutants. Cells used in (B) were cultured in the presence or absence of 500 ng/ml of MMC for 6 hr before microscopic observation.

GFP-Mcm9 mutants (Figure S3C). These results suggest that the ATPase activity of the Mcm8-9 complex is required for the efficient formation of foci.

The Mcm8 and Mcm9 Complex Functions Downstream of the FA and BRCA2/Rad51 Pathways

Reminiscent of what is observed in FA cells, *mcm8*^{KO} and *mcm9*^{KO} cells were hypersensitive to ICL-inducing agents and exhibited chromosome aberrations after MMC treatment (Figures 2B and 2C). FANCD2 monounbiquitylation, which is catalyzed by the FA core complex, is a hallmark of the activation of the FA pathway (Garcia-Higuera et al., 2001). To investigate whether the Mcm8-9 complex plays a role upstream of the FA pathway, we studied FANCD2 monoubiquitylation in *mcm8*^{KO} and *mcm9*^{KO} cells (Figure 5A). In wild-type cells, higher levels of a slow-migrating FANCD2 (FANCD2-L), representing the monoubiquitylation form, were induced in the presence of MMC (Figure 5A, WT, +MMC). FANCD2-L was lost in cells lacking FANCC (Figure 5A, *fancc*^{KO}, +MMC) (Garcia-Higuera et al., 2001; Hirano et al., 2005; Niedzwiedz et al., 2004). The level of FANCD2-L was not affected in *mcm8*^{KO} and *mcm9*^{KO} cells (Figure 5A, *mcm8*^{KO} and *mcm9*^{KO}, +MMC), indicating that Mcm8 and Mcm9 do not play a role upstream of the FA core complex. The checkpoint mediator Chk1 was phosphorylated normally after addition of MMC (Figure 5B, phospho-Chk1), showing that Mcm8 and Mcm9 are not involved in checkpoint activation. Taken together, these results indicate that the Mcm8-9 complex plays a role either downstream of FANCD2 or independent of the FA pathway.

Please cite this article in press as: Nishimura et al., Mcm8 and Mcm9 Form a Complex that Functions in Homologous Recombination Repair Induced by DNA Interstrand Crosslinks, Molecular Cell (2012), http://dx.doi.org/10.1016/j.molcel.2012.05.047

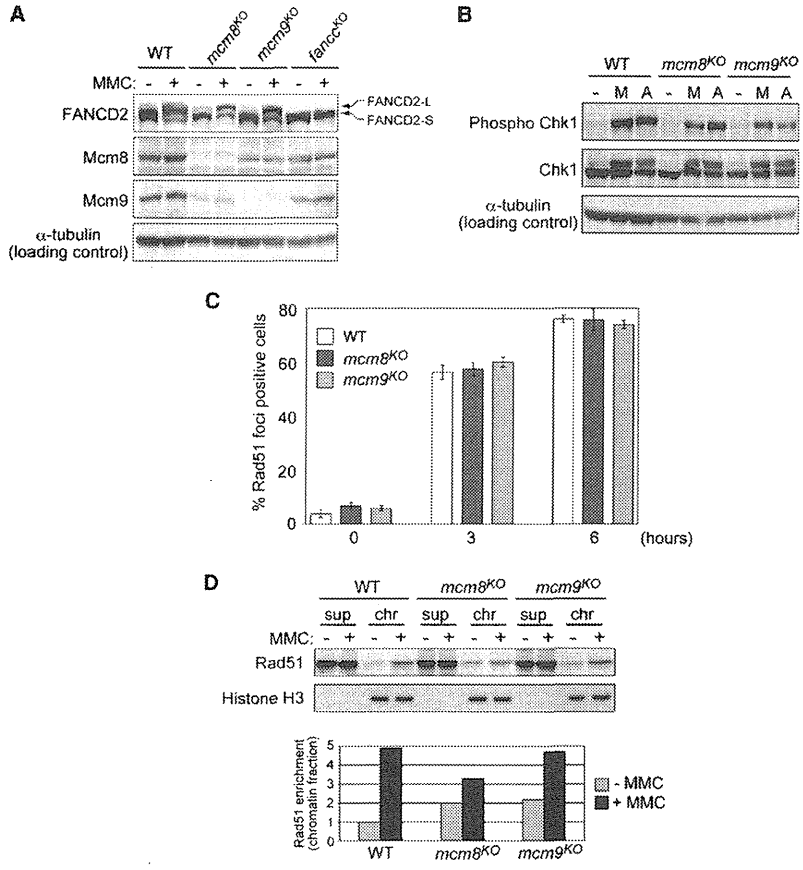

Figure 5. Mcm8 and Mcm9 Are Not Required for the Activation of FA Pathway and for Rad51 Loading

(A) Immunoblot detection of FANCD2-L after MMC treatment. Indicated cells were cultured in the presence or absence of 500 ng/ml of MMC for 6 hr. The indicated proteins were detected by immunoblotting using specific antibodies.

(B) Immunoblot detection of Chk1 phosphorylation after MMC treatment. Indicated cells were mock treated (–) or cultured in the presence of 500 ng/ml MMC (M) or 6 μg/ml aphidicolin (A) for 6 hr. Extracts were processed via immunoblotting using specific antibodies against the indicated proteins.

(C) Formation of Rad51 foci in wild-type, *mcm8*^{KO}, and *mcm9*^{KO} cells after MMC treatment. The cells were fixed at an indicated time after incubation in the presence of 500 ng/ml of MMC. The cells containing more than five Rad51 nuclear foci were counted as positive. More than 50 cells were scored. Error bars indicate SD.

(D) MMC-induced Rad51 chromatin association in wild-type, *mcm8*^{KO}, and *mcm9*^{KO} cells. Indicated cells were treated as in (A). After centrifugal fractionation, Rad51 was detected by immnoblotting. Histone H3 was also detected as a control showing chromatin fraction. Rad51 found in chromatin fraction was quantified (bar graph).

In parallel to the FA pathway, Rad51 is loaded around ICLs for subsequent HR repair (Godthelp et al., 2002; Kitao et al., 2006; Long et al., 2011). Therefore, we investigated whether Mcm8 and Mcm9 are required for Rad51 loading. Wild-type, *mcm8*^{KO}, and *mcm9*^{KO} cells were cultured in the presence of MMC before microscopic observation of Rad51 foci. Rad51 foci were formed in cells lacking Mcm8 and Mcm9 (Figure S4A), and the kinetics of the formation of foci was indistinguishable among the cell lines (Figure 5C), showing that Mcm8 and Mcm9 are not required for Rad51 loading. We also analyzed chromatin association of Rad51 in the presence or absence of MMC (Figure 5D). In wild-type cells, Rad51 association to chromatin increased to 4.9 times upon MMC treatment (Figure 5D, WT) (Kitao et al., 2006). In *mcm8*^{KO} or *mcm9*^{KO} cells, MMC treatment induced chromatin association of Rad51 to 3.3 and 4.7 times, respectively, compared to that in wild-type cells without MMC (Figure 5D, *mcm8*^{KO} or *mcm9*^{KO}). We noticed that more Rad51 associated to chromatin even without MMC, reflecting the fact that they have a defect in proliferation possibly by the accumulation of DNA damage (Figure 2A and Figure S2B). We conclude that the Mcm8-9 complex is not required for Rad51 loading.

Next, we determined whether the Mcm8-9 complex acts downstream of the FA pathway. To address this question, the formation of GFP-Mcm9 foci after MMC treatment was investigated. We introduced *GFP-MCM9* stably into wild-type cells or into cells that were deficient in FANCD2 (*fancd2*^{KO}) (Yamamoto et al., 2005). The MMC-dependent formation of GFP-Mcm9 foci was observed in the wild-type background, showing that ectopically expressed GFP-Mcm9 functions in the presence of endogenous Mcm9, as was the case in the *mcm9*^{KO} background (Figures 6A and 6B, WT). We found that the MMC-induced formation of GFP-Mcm9 foci was severely diminished in *fancd2*^{KO} cells (Figures 6A and 6B, *fancd2*^{KO}). We also observed a similar loss of GFP-Mcm9 foci in *fancd2*^{KR} (expressing a nonubiquitylation form of FANCD2) and *fancc*^{KO} cells (Figures S4B and S4C) (Hirano et al., 2005; Seki et al., 2007). These results strongly suggest that the Mcm8-9 complex operates in a process that takes place downstream of the FA pathway.

Subsequently, we investigated whether BRCA2/Rad51 pathway is required for the MMC-dependent formation of GFP-Mcm9 foci. We stably expressed GFP-Mcm9 in *brca2*$^{\Delta CTD/con}$ cells, which express a C-terminally truncated BRCA2 protein mimicking the defective allele of FANCD1 patients and a conditional BRCA2, the encoding gene of which is excised after addition of orthohydroxytamoxifen (OHT) (Kitao et al., 2006). In these cells, the MMC-induced Rad51 foci were mostly lost after OHT addition (Figure S4D). The MMC-induced GFP-Mcm9 foci were significantly reduced after treatment with OHT (Figures 6C and 6D). These results suggest that the Mcm8-9 complex functions in a process that takes place downstream of the

Please cite this article in press as: Nishimura et al., Mcm8 and Mcm9 Form a Complex that Functions in Homologous Recombination Repair Induced by DNA Interstrand Crosslinks, Molecular Cell (2012), http://dx.doi.org/10.1016/j.molcel.2012.05.047

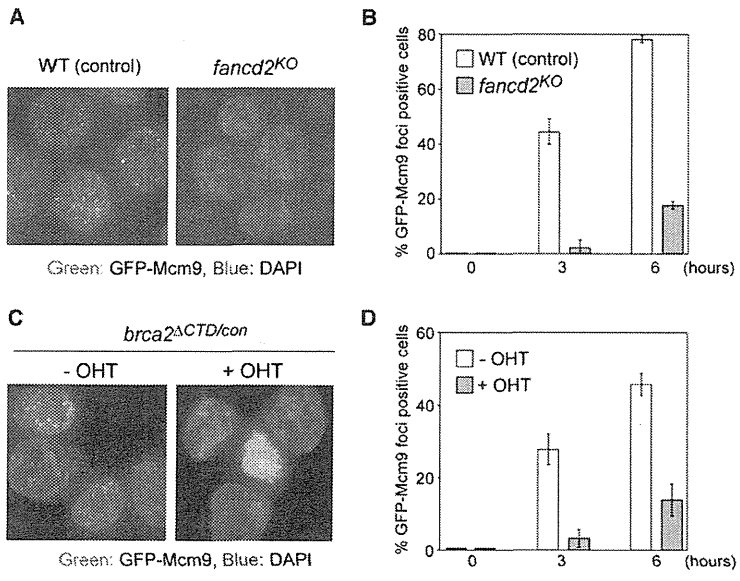

Figure 6. The Mcm8-9 Complex Functions Downstream of the FA and BRCA2/Rad51 Pathways

(A) Formation of GFP-Mcm9 foci in cells lacking FANCD2. The indicated cells expressing GFP-Mcm9 were fixed at 6 hr after addition of 500 ng/ml of MMC.

(B) The cells used in (A) were fixed at 0, 3, and 6 hr. Cells containing more than five GFP-Mcm9 nuclear foci were considered positive. More than 50 cells were scored. Error bars indicate SD.

(C) Formation of GFP-Mcm9 foci in cells lacking functional BRCA2. The indicated cells expressing GFP-Mcm9 were fixed at 6 hr after addition of 500 ng/ml of MMC.

(D) The cells used in (C) were fixed at 0, 3, and 6 hr. Cells containing more than five GFP-Mcm9 nuclear foci were considered positive. More than 50 cells were scored. Error bars indicate SD.

BRCA2/Rad51 pathway. Although there was a clear difference in the kinetics of these cells compared with that of wild-type cells, the percentage of *fancd2*^{KO} and *brca2*$^{\Delta CTD/con}$ (+ OHT) cells that were positive for Mcm8 and Mcm9 foci increased at 6 hr (Figures 6B and 6D), suggesting the existence of an alternative pathway for Mcm8-9 loading. Taken together, these results lead us to conclude that the Mcm8-9 complex functions in a process that takes place downstream of the FA and BRCA2/Rad51 pathways.

Mcm8 and Mcm9 Are Involved in HR

HR repair is expected after FA activation and Rad51 loading. Therefore, we investigated whether the Mcm8-9 complex is involved in HR. To address this question, we initially assessed the frequency of HR-mediated recombination repair induced by I-SceI in wild-type and *mcm8*^{KO} cells (Johnson et al., 1999; Yamamoto et al., 2005). We found that the I-SceI-dependent recombination frequency was reduced to less than one-tenth in *mcm8*^{KO} cells, strongly suggesting that Mcm8 is involved in HR (Figure 7A). Subsequently, we studied HR-mediated targeting efficiencies in wild-type, *mcm8*^{KO}, and *mcm9*^{KO} cells (Figure 7B). We transfected targeting constructs designed to insert a selection marker at the *ovalbumin* and *CENP-H* loci for wild-type, *mcm8*^{KO}, and *mcm9*^{KO} cells (Buerstedde and Takeda, 1991; Fukagawa et al., 2001) as well as at the *MCM9* locus for wild-type and *mcm8*^{KO} cells. In all cases, the targeting frequencies in *mcm8*^{KO} and *mcm9*^{KO} cells were significantly reduced, suggesting that Mcm8 and Mcm9 are involved in a pathway that is required for HR-mediated targeting. Further, HR-dependent gene conversion of the Ig V locus in the surface IgM (sIgM) gene was measured in wild-type, *mcm8*^{KO}, and *mcm9*^{KO} cells (Figure S5A). We cultured 20 sIgM-positive subclones for 18 days before quantification of sIgM-negative cells in the population. Compared to wild-type subclones, significantly and slightly fewer sIgM-negative cells were found in the *mcm8*^{KO} and *mcm9*^{KO} subclones, respectively, suggesting that Mcm8 and Mcm9 function in the gene conversion.

All results shown above support the idea that the Mcm8-9 complex is involved in HR. Then we asked whether Mcm8 and Mcm9 promote SCEs as a consequence of HR repair during DNA replication (Sonoda et al., 1999). Intriguingly, both spontaneous and MMC-induced SCE levels in *mcm8*^{KO} and *mcm9*^{KO} cells were significantly reduced (Figure 7C, *mcm8*^{KO} and *mcm9*^{KO}), similar to the case with the cell deficient in the Rad51 paralog *XRCC3* (Figure 7C, *xrcc3*^{KO}) (Takata et al., 2001). Taken together, we concluded that the Mcm8-9 complex functions in ICL-induced HR repair that promotes SCEs, possibly as a hexameric ATPase/helicase complex (Figure S5B).

DISCUSSION

Nonessential Mcm Proteins in Other Organisms

Our study revealed that Mcm8 and Mcm9 form a complex that is not essential for cell viability in chicken DT40 cells. Even though Mcm8 and Mcm9 are involved in DNA replication in humans and *Xenopus* (Lutzmann and Mechali, 2008; Maiorano et al., 2005; Volkening and Hoffmann, 2005), their roles in replication must be nonessential in DT40 cells. In agreement with the results of our study, a recent report showed that Mcm9 is dispensable in mice (Hartford et al., 2011). In *Drosophila*, which does not have *MCM9*, *MCM8/REC* is also not essential for viability (Blanton et al., 2005; Matsubayashi and Yamamoto, 2003). Thus, it is likely that Mcm8 and Mcm9 are not essential for DNA replication in other organisms. Recently, two reports showed that the archaea, *Thermococcus kodakarensis*, has three Mcm family proteins, TkoMcm1, TkoMcm2, and TkoMcm3, among which TkoMcm1 and TkoMcm2 are not essential for cell viability (Ishino et al., 2011; Pan et al., 2011). We noticed that both TkoMcm1 and 2 have a Walker A consensus sequence similar to what is observed in Mcm8 and Mcm9 rather than in Mcm2-7 (Figure S6A). A recent phylogenetic analysis of the proteins of the Mcm family suggested that the last common ancestor of eukaryotic cells had both Mcm8 and Mcm9 (Liu et al., 2009). Therefore, archaeal TkoMcm1 and/or TkoMcm2 may be the functional homolog of eukaryotic Mcm8 and Mcm9.

Please cite this article in press as: Nishimura et al., Mcm8 and Mcm9 Form a Complex that Functions in Homologous Recombination Repair Induced by DNA Interstrand Crosslinks, Molecular Cell (2012), http://dx.doi.org/10.1016/j.molcel.2012.05.047

A

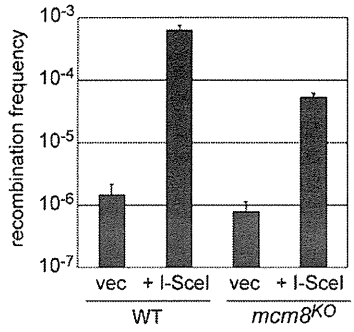

B

Genotype	Frequency (%) for targeting construct		
	ovalbumin	*CENP-H*	*MCM9*
WT (control)	5/25 (20%)	17/30 (56.7%)	17/33 (51.5%)
mcm8^{KO}	0/27 (0%)	1/26 (3.8%)	2/31 (6.5%)
mcm9^{KO}	0/20 (0%)	3/25 (12%)	——

C

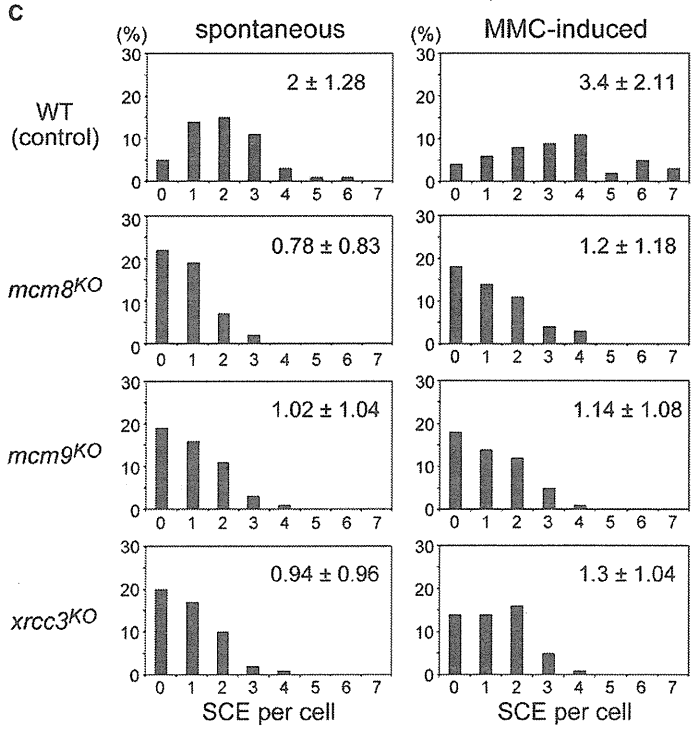

Figure 7. The Mcm8-9 Complex Is Involved in HR

(A) I-SceI-induced recombination frequencies in wild-type and *mcm8^{KO}* cells. Wild-type or *mcm8^{KO}* cells containing one copy of the *SCneo* substrate at the ovalbumin locus were transfected with pBluescript (vec) or I-SceI expression vector (+I-SceI) by electroporation. Cells were selected in medium containing 2.0 mg/ml G418, and surviving colonies were counted after 10 days. Mean ± SD of three independent experiments is shown.

(B) HR-mediated gene targeting frequencies in wild-type, *mcm8^{KO}*, and *mcm9^{KO}* cells.

(C) Distribution of spontaneous and MMC-induced SCEs in wild-type, *mcm8^{KO}*, *mcm9^{KO}*, and *xrcc3^{KO}* cells. After labeling with 10 μM BrdU for 12 hr, cells were either mock treated or treated with 50 ng/ml MMC for 6 hr. Mean ± SD of scores from 50 metaphases is also indicated.

Consistent with the formation of the Mcm8-9 complex, the level of each of these proteins depended on the level of the other (Figure 1A, Figure 5A, and Figures S3A and S3B). Interestingly, Mcm8 was less affected in the absence of Mcm9. Indeed, *mcm8^{KO}* and *mcm9^{KO}* cells exhibited similar phenotypes in general; however, *mcm8^{KO}* cells showed slightly higher IR and UV sensitivities (Figures 2B). Moreover, *mcm8^{KO}* cells showed lower gene targeting and HR-mediated IgM conversion frequencies compared to *mcm9^{KO}* cells (Figure 7B and Figure S5A). Taking into account the possibility that *Drosophila* Mcm8/REC may have evolved to function in the absence of Mcm9 (Liu et al., 2009), Mcm8 may be able to function without Mcm9 to some extent in vertebrates.

Why do some eukaryotic organisms lack both Mcm8 and Mcm9? A possible explanation is that those organisms have redundant mechanisms for repairing ICLs. ICLs are efficiently repaired in the G1 phase using a combination of NER and TLS without HR in budding yeast (Barber et al., 2005; Sarkar et al., 2006). Interestingly, the *MCM8* and *MCM9* genes either coexist or codisappear in eukaryotes, with the exception of *Drosophila* (Liu et al., 2009), and organisms lacking Mcm8 and Mcm9 have relatively smaller genomes (Figure S6B). It can be assumed that the Mcm8-9 complex is more important for maintaining genomic integrity in organisms with a large genome. For these reasons, Mcm8 and Mcm9 may have been lost in organisms such as yeasts.

Role of the Mcm8-9 Complex in ICL-Induced HR Repair

Because ICL repair is initiated after the stalling of the replication fork at ICLs, a defect in DNA replication caused by the loss of Mcm8 or Mcm9 may affect ICL repair. However, four lines of evidence support our conclusion that the Mcm8-9 complex is directly involved in ICL repair. First, *mcm8^{KO}* and *mcm9^{KO}* cells were not hypersensitive to non-ICL damage including replication stress caused by HU and aphidicolin

Please cite this article in press as: Nishimura et al., Mcm8 and Mcm9 Form a Complex that Functions in Homologous Recombination Repair Induced by DNA Interstrand Crosslinks, Molecular Cell (2012), http://dx.doi.org/10.1016/j.molcel.2012.05.047

(Figure 2B and Figure S2C). Second, checkpoint activation and FANCD2 monoubiquitylation induced by MMC were unaffected (Figures 5A and 5B), suggesting that replication forks were generated normally. Third, we found that the MMC-induced Mcm9 foci were diminished in both *fancd2*^{KO} and *brca2*^{4CTD} cells (Figure 6). Fourth, both Mcm8 and Mcm9 were involved in HR (Figure 7 and Figure S5A). Thus, we conclude that the Mcm8-9 complex is directly involved in ICL repair by playing a role in a Rad51-dependent HR repair process that takes place downstream of the FA proteins (Figure S5B).

A likely hypothesis is that the Mcm8-9 complex is a hexameric helicase that plays a role after Rad51 loading during ICL-induced HR repair. As a DNA helicase, the Mcm8-9 complex may be involved in the repair synthesis after strand invasion or the branch migration of the Holliday structure. GFP-Mcm9 foci that did not colocalize with Rad51 might represent the Mcm8-9 complex functioning after strand invasion (Figure 3B). Because Mcm8 and Mcm9 were required for efficient HR (Figure 7 and Figure S5A), we favor the idea that the Mcm8-9 complex is also involved in other HR repairs. However, a subpathway in other HR repair that does not require Mcm8-9 may be able to work in such cases, with the result that *mcm8*^{KO} and *mcm9*^{KO} were not highly sensitive to IR (Figure 2B). Studies performed using *Xenopus* egg extracts showed that an ICL in plasmids is repaired when two replication forks are encountered at the ICL (Raschle et al., 2008), resulting in the generation of a double-ended DSB similar to that observed for the IR-induced DSBs. Although such two-fork encounters at ICLs likely occur as cells complete replication in the late S phase, we do not know their actual frequency in cells. In the early to mid-S phase, a stalled fork at ICLs from one direction is more likely to be processed, to generate a one-ended DSB. Because replication forks have to be regenerated, HR repair induced by a one-ended DSB must be mechanistically distinct from that induced by a two-ended DSB. Taking into account the observation that the *mcm8*^{KO} and *mcm9*^{KO} cells were hypersensitive to ICL-inducing agents, but not to IR (Figure 2B), the Mcm8-9 complex may play an important role in the HR repair induced by a one-ended DSB.

Our conclusion that both Mcm8 and Mcm9 are involved in HR repair provides a good explanation for the recent finding that *mcm9* mutant mice exhibit a cancer-susceptible phenotype (Hartford et al., 2011). The authors in the same report found that female mice expressing a truncated Mcm9 have fewer follicles in ovaries, and oocytes are lost by 24 weeks after birth. A genome-wide screening showed that SNPs located in the *MCM8* gene are associated with the age of natural menopause of human females (He et al., 2009). These independent findings suggest that the Mcm8-9 complex functions in the growth of germ stem cells and/or meiosis. Taking into account that *Drosophila* Mcm8/REC is involved in meiotic recombination (Blanton et al., 2005; Matsubayashi and Yamamoto, 2003), it will be interesting to investigate whether the Mcm8-9 complex plays a role in meiotic recombination.

In summary, we showed that Mcm8 and Mcm9 form a complex that is involved in ICL-induced HR repair. Furthermore, our results imply the existence of a unique HR system involving the Mcm8-9 complex that is important for ICL repair in vertebrate cells.

EXPERIMENTAL PROCEDURES

DT40 Cell Growth and Gene Targeting

Chicken DT40 cells were cultured in DMEM/high glucose medium (Sigma) supplemented with 10^{-5} M β-mercaptoethanol (Sigma), 100 U/ml penicillin and 100 μg/ml streptomycin (GIBCO), 10% fetal calf serum (Hana-Nesco Bio), and 1% chicken serum (GIBCO) at 38.5°C. Cells were counted using a TC10 cell counter (Bio-Rad). All plasmids were constructed using standard methods. Chicken *MCM8* and *MCM9* cDNAs (accession numbers AB689140 and AB689141, respectively) were amplified from an RT-PCR library of DT40 total RNA. To construct plasmids for the FLAG- and GFP-fusion expression, p3xFLAG-CMV-10 (Sigma) and pEGFP-C1 (Clontech) plasmids were used, respectively. The structure of *MCM8* and *MCM9* knockout plasmids is illustrated in Figures S1B and S1E. DT40 cells were transfected and selected as described previously (Buerstedde and Takeda, 1991).

Cell-Viability Assay

Serially diluted cells were plated into medium containing 1.5% methylcellulose. To study IR sensitivity, the indicated dose of IR was irradiated soon after plating. MMS or cisplatin sensitivity was tested by the addition of each drug into the methylcellulose medium. To mesure MMC sensitivity, exponentially growing cells were incubated in medium containing MMC for 1 hr before washing and releasing into methylcellulose medium without MMC. Colonies were counted after incubation for 1–2 weeks.

Protein Detection

Cells were lysed in the Laemmli sample buffer before lysates were cleared through a 0.45 μm Nylon filter (Spin-X centrifuge tube filter, Coster). After denaturation at 95°C for 5 min, equal amounts of total protein were separated using SDS-PAGE. Proteins were transferred to a Hybond ECL membrane (GE Healthcare) and blotted with antibodies after blocking in TBST containing 10% skim milk for 1 hr at RT. Detection was performed using the ECL prime reagents (GE Healthcare) with an ImageQuant LAS400 mini system (GE Healthcare). To raise rabbit polyclonal antibodies against chicken Mcm8 and Mcm9, the Strep-tag-fused Mcm8 (aa 1–380) and Mcm9 (aa 876–1170) fragments were expressed in *E. coli* and were purified using Strep-Tactin beads (IBA). The exclusive detection of the target protein, and not of other Mcm family proteins, by the antibodies produced was confirmed.

Gel Filtration Assay

Exponentially growing wild-type cells (2×10^7) were lysed in 1 ml of Lysis buffer (20 mM HEPES-KOH [pH 7.9], 100 mM KOAc, 0.1% Triton X-100, 1 mM EDTA, 1× Complete EDTA free protease inhibitor mix [Roche], 1× phosSTOP phosphatase inhibitor mix [Roche]). Crude extracts were sonicated and cleared through a 0.45 μm disk filter to remove insoluble materials. Extracts were fractionated through a Superose 6 10/300 GL column attached to an ATKAexplorer 100 system (GE Healthcare).

Immunoprecipitation Assay

Exponentially growing cells (1×10^8) were lysed in 5 ml of IP buffer (20 mM HEPES-KOH [pH 7.9], 300 mM NaCl, 2.5 mM $CaCl_2$, 0.1% Triton X-100, 5 mM β-mercaptoethanol, 1× Complete EDTA free protease inhibitor mix [Roche], 1× PhosSTOP phosphatase inhibitor mix [Roche]). Crude extracts were sonicated before adding 750 U of MNase (Roche). Extracts were incubated on ice for 1 hr to digest DNA. After ultracentrifugation at 30 krpm for 1 hr at 4°C using an MLS-50 rotor (Beckman), supernatants were collected and mixed with anti-FLAG M2 agarose (Sigma) or anti-Mcm9-coated protein A magnetic beads (Life Technologies). After continuous agitation for 1 hr at 4°C, the beads were extensively washed (five times) with IP buffer. Bound proteins were eluted with IP buffer containing 200 μg/ml of the 3× FLAG peptide (Sigma) or with Laemmli sample buffer.

Microscopy

Cells were fixed with 4% paraformaldehyde for 30 min at RT before permeabilization with PBS containing 0.5% Triton-X for 30 min. Treated cells were immobilized on glass slides using a cytospin. To detect Rad51, cells were treated with an anti-Rad51 polyclonal antibody at 37°C for 1 hr after blocking with PBS

containing 1% BSA at RT for 30 min; subsequently, cells were treated with an Alexa Fluor 594-conjugated anti-rabbit IgG (Molecular Probes) at 37°C for 1 hr. After staining with DAPI, samples were analyzed under a DeltaVision microscope (Applied Precision). Chromosome analysis was performed as described previously (Takata et al., 2000, 2001).

Flow Cytometry

DT40 cells were pulse labeled with 20 μM BrdU for 20 min before fixation with ice-cold 70% ethanol. After treatment with 4 M HCl containing 0.5% Triton-X for 30 min, cells were incubated with an anti-BrdU antibody (BD) for 1 hr at RT and then with an FITC-conjugated anti-mouse IgG (Jackson ImmunoResearch Laboratories) at RT for 30 min. Cells were stained with 5 μg/ml of propidium iodide in PBS and analyzed using a FACSCalibur machine (BD).

I-SceI-Induced HR and sIgM Conversion Assays

These assays were performed as described previously (Yamamoto et al., 2005).

ACCESSION NUMBERS

The accession numbers for the chicken *MCM8* and *MCM9* sequences reported in this paper are AB689140 and AB689141, respectively.

SUPPLEMENTAL INFORMATION

Supplemental Information includes six figures and can be found with this article online at http://dx.doi.org/10.1016/j.molcel.2012.05.047.

ACKNOWLEDGMENTS

We thank Hiroyuki Araki (National Institute of Genetics) for critical reading of the manuscript, Akemi Mizuguchi (National Institute of Genetics) for experimental support, and Anindya Dutta (University of Virginia) for sharing unpublished data. We also thank Hitoshi Kurumizaka (Waseda University) for providing the anti-Rad51 antibody. K.N. is a JSPS postdoctoral fellow (PD). This work was funded by grants from the Ministry of Education, Science, Sports, and Culture of Japan.

Received: January 24, 2012
Revised: May 14, 2012
Accepted: May 31, 2012
Published online: July 5, 2012

REFERENCES

Akkari, Y.M., Bateman, R.L., Reifsteck, C.A., Olson, S.B., and Grompe, M. (2000). DNA replication is required to elicit cellular responses to psoralen-induced DNA interstrand cross-links. Mol. Cell. Biol. *20*, 8283–8289.

Barber, L.J., Ward, T.A., Hartley, J.A., and McHugh, P.J. (2005). DNA interstrand cross-link repair in the Saccharomyces cerevisiae cell cycle: overlapping roles for PSO2 (SNM1) with MutS factors and EXO1 during S phase. Mol. Cell. Biol. *25*, 2297–2309.

Blanton, H.L., Radford, S.J., McMahan, S., Kearney, H.M., Ibrahim, J.G., and Sekelsky, J. (2005). REC, Drosophila MCM8, drives formation of meiotic crossovers. PLoS Genet. *1*, e40. http://dx.doi.org/10.1371/journal.pgen.0010040.

Bochman, M.L., and Schwacha, A. (2008). The Mcm2-7 complex has in vitro helicase activity. Mol. Cell *31*, 287–293.

Bochman, M.L., and Schwacha, A. (2009). The Mcm complex: unwinding the mechanism of a replicative helicase. Microbiol. Mol. Biol. Rev. *73*, 652–683.

Bochman, M.L., Bell, S.P., and Schwacha, A. (2008). Subunit organization of Mcm2-7 and the unequal role of active sites in ATP hydrolysis and viability. Mol. Cell. Biol. *28*, 5865–5873.

Buerstedde, J.M., and Takeda, S. (1991). Increased ratio of targeted to random integration after transfection of chicken B cell lines. Cell *67*, 179–188.

Davey, M.J., Indiani, C., and O'Donnell, M. (2003). Reconstitution of the Mcm2-7p heterohexamer, subunit arrangement, and ATP site architecture. J. Biol. Chem. *278*, 4491–4499.

Deans, A.J., and West, S.C. (2011). DNA interstrand crosslink repair and cancer. Nat. Rev. Cancer *11*, 467–480.

Fukagawa, T., Mikami, Y., Nishihashi, A., Regnier, V., Haraguchi, T., Hiraoka, Y., Sugata, N., Todokoro, K., Brown, W., and Ikemura, T. (2001). CENP-H, a constitutive centromere component, is required for centromere targeting of CENP-C in vertebrate cells. EMBO J. *20*, 4603–4617.

Garcia-Higuera, I., Taniguchi, T., Ganesan, S., Meyn, M.S., Timmers, C., Hejna, J., Grompe, M., and D'Andrea, A.D. (2001). Interaction of the Fanconi anemia proteins and BRCA1 in a common pathway. Mol. Cell *7*, 249–262.

Godthelp, B.C., Artwert, F., Joenje, H., and Zdzienicka, M.Z. (2002). Impaired DNA damage-induced nuclear Rad51 foci formation uniquely characterizes Fanconi anemia group D1. Oncogene *21*, 5002–5005.

Gozuacik, D., Chami, M., Lagorce, D., Faivre, J., Murakami, Y., Poch, O., Biermann, E., Knippers, R., Brechot, C., and Paterlini-Brechot, P. (2003). Identification and functional characterization of a new member of the human Mcm protein family: hMcm8. Nucleic Acids Res. *31*, 570–579.

Hanada, K., Budzowska, M., Modesti, M., Maas, A., Wyman, C., Essers, J., and Kanaar, R. (2006). The structure-specific endonuclease Mus81-Eme1 promotes conversion of interstrand DNA crosslinks into double-strands breaks. EMBO J. *25*, 4921–4932.

Hanson, P.I., and Whiteheart, S.W. (2005). AAA+ proteins: have engine, will work. Nat. Rev. Mol. Cell Biol. *6*, 519–529.

Hartford, S.A., Luo, Y., Southard, T.L., Min, I.M., Lis, J.T., and Schimenti, J.C. (2011). Minichromosome maintenance helicase paralog MCM9 is dispensible for DNA replication but functions in germ-line stem cells and tumor suppression. Proc. Natl. Acad. Sci. USA *108*, 17702–17707.

He, C., Kraft, P., Chen, C., Buring, J.E., Pare, G., Hankinson, S.E., Chanock, S.J., Ridker, P.M., Hunter, D.J., and Chasman, D.I. (2009). Genome-wide association studies identify loci associated with age at menarche and age at natural menopause. Nat. Genet. *41*, 724–728.

Hirano, S., Yamamoto, K., Ishiai, M., Yamazoe, M., Seki, M., Matsushita, N., Ohzeki, M., Yamashita, Y.M., Arakawa, H., Buerstedde, J.M., et al. (2005). Functional relationships of FANCC to homologous recombination, translesion synthesis, and BLM. EMBO J. *24*, 418–427.

Ilves, I., Petojevic, T., Pesavento, J.J., and Botchan, M.R. (2010). Activation of the MCM2-7 helicase by association with Cdc45 and GINS proteins. Mol. Cell *37*, 247–258.

Ishino, S., Fujino, S., Tomita, H., Ogino, H., Takao, K., Daiyasu, H., Kanai, T., Atomi, H., and Ishino, Y. (2011). Biochemical and genetical analyses of the three mcm genes from the hyperthermophilic archaeon, Thermococcus kodakarensis. Genes Cells *16*, 1176–1189.

Johnson, R.D., Liu, N., and Jasin, M. (1999). Mammalian XRCC2 promotes the repair of DNA double-strand breaks by homologous recombination. Nature *401*, 397–399.

Johnson, E.M., Kinoshita, Y., and Daniel, D.C. (2003). A new member of the MCM protein family encoded by the human MCM8 gene, located contrapodal to GCD10 at chromosome band 20p12.3-13. Nucleic Acids Res. *31*, 2915–2925.

Kawabata, T., Luebben, S.W., Yamaguchi, S., Ilves, I., Matise, I., Buske, T., Botchan, M.R., and Shima, N. (2011). Stalled fork rescue via dormant replication origins in unchallenged S phase promotes proper chromosome segregation and tumor suppression. Mol. Cell *41*, 543–553.

Kee, Y., and D'Andrea, A.D. (2010). Expanded roles of the Fanconi anemia pathway in preserving genomic stability. Genes Dev. *24*, 1680–1694.

Kitao, H., Yamamoto, K., Matsushita, N., Ohzeki, M., Ishiai, M., and Takata, M. (2006). Functional interplay between BRCA2/FancD1 and FancC in DNA repair. J. Biol. Chem. *281*, 21312–21320.

Liu, N., Lamerdin, J.E., Tebbs, R.S., Schild, D., Tucker, J.D., Shen, M.R., Brookman, K.W., Siciliano, M.J., Walter, C.A., Fan, W., et al. (1998). XRCC2 and XRCC3, new human Rad51-family members, promote chromosome

stability and protect against DNA cross-links and other damages. Mol. Cell *1*, 783–793.

Liu, Y., Richards, T.A., and Aves, S.J. (2009). Ancient diversification of eukaryotic MCM DNA replication proteins. BMC Evol. Biol. *9*, 60. http://dx.doi.org/10.1186/1471-2148-9-60.

Long, D.T., Raschle, M., Joukov, V., and Walter, J.C. (2011). Mechanism of RAD51-dependent DNA interstrand cross-link repair. Science *333*, 84–87.

Lutzmann, M., and Mechali, M. (2008). MCM9 binds Cdt1 and is required for the assembly of prereplication complexes. Mol. Cell *31*, 190–200.

Lutzmann, M., Maiorano, D., and Mechali, M. (2005). Identification of full genes and proteins of MCM9, a novel, vertebrate-specific member of the MCM2-8 protein family. Gene *362*, 51–56.

Maiorano, D., Cuvier, O., Danis, E., and Mechali, M. (2005). MCM8 is an MCM2-7-related protein that functions as a DNA helicase during replication elongation and not initiation. Cell *120*, 315–328.

Matsubayashi, H., and Yamamoto, M.T. (2003). REC, a new member of the MCM-related protein family, is required for meiotic recombination in Drosophila. Genes Genet. Syst. *78*, 363–371.

Moldovan, G.L., and D'Andrea, A.D. (2009). How the Fanconi anemia pathway guards the genome. Annu. Rev. Genet. *43*, 223–249.

Niedernhofer, L.J., Odijk, H., Budzowska, M., van Drunen, E., Maas, A., Theil, A.F., de Wit, J., Jaspers, N.G., Beverloo, H.B., Hoeijmakers, J.H., et al. (2004). The structure-specific endonuclease Ercc1-Xpf is required to resolve DNA interstrand cross-link-induced double-strand breaks. Mol. Cell. Biol. *24*, 5776–5787.

Niedzwiedz, W., Mosedale, G., Johnson, M., Ong, C.Y., Pace, P., and Patel, K.J. (2004). The Fanconi anaemia gene FANCC promotes homologous recombination and error-prone DNA repair. Mol. Cell *15*, 607–620.

Pan, M., Santangelo, T.J., Li, Z., Reeve, J.N., and Kelman, Z. (2011). Thermococcus kodakarensis encodes three MCM homologs but only one is essential. Nucleic Acids Res. *39*, 9671–9680.

Raschle, M., Knipscheer, P., Enoiu, M., Angelov, T., Sun, J., Griffith, J.D., Ellenberger, T.E., Scharer, O.D., and Walter, J.C. (2008). Mechanism of replication-coupled DNA interstrand crosslink repair. Cell *134*, 969–980.

Sarkar, S., Davies, A.A., Ulrich, H.D., and McHugh, P.J. (2006). DNA interstrand crosslink repair during G1 involves nucleotide excision repair and DNA polymerase zeta. EMBO J. *25*, 1285–1294.

Sasaki, M.S., and Tonomura, A. (1973). A high susceptibility of Fanconi's anemia to chromosome breakage by DNA cross-linking agents. Cancer Res. *33*, 1829–1836.

Schwacha, A., and Bell, S.P. (2001). Interactions between two catalytically distinct MCM subgroups are essential for coordinated ATP hydrolysis and DNA replication. Mol. Cell *8*, 1093–1104.

Seki, S., Ohzeki, M., Uchida, A., Hirano, S., Matsushita, N., Kitao, H., Oda, T., Yamashita, T., Kashihara, N., Tsubahara, A., et al. (2007). A requirement of FancL and FancD2 monoubiquitination in DNA repair. Genes Cells *12*, 299–310.

Simpson, L.J., and Sale, J.E. (2003). Rev1 is essential for DNA damage tolerance and non-templated immunoglobulin gene mutation in a vertebrate cell line. EMBO J. *22*, 1654–1664.

Sonoda, E., Sasaki, M.S., Morrison, C., Yamaguchi-Iwai, Y., Takata, M., and Takeda, S. (1999). Sister chromatid exchanges are mediated by homologous recombination in vertebrate cells. Mol. Cell. Biol. *19*, 5166–5169.

Sonoda, E., Okada, T., Zhao, G.Y., Tateishi, S., Araki, K., Yamaizumi, M., Yagi, T., Verkaik, N.S., van Gent, D.C., Takata, M., et al. (2003). Multiple roles of Rev3, the catalytic subunit of polzeta in maintaining genome stability in vertebrates. EMBO J. *22*, 3188–3197.

Takata, M., Sasaki, M.S., Sonoda, E., Fukushima, T., Morrison, C., Albala, J.S., Swagemakers, S.M., Kanaar, R., Thompson, L.H., and Takeda, S. (2000). The Rad51 paralog Rad51B promotes homologous recombinational repair. Mol. Cell. Biol. *20*, 6476–6482.

Takata, M., Sasaki, M.S., Tachiiri, S., Fukushima, T., Sonoda, E., Schild, D., Thompson, L.H., and Takeda, S. (2001). Chromosome instability and defective recombinational repair in knockout mutants of the five Rad51 paralogs. Mol. Cell. Biol. *21*, 2858–2866.

Volkening, M., and Hoffmann, I. (2005). Involvement of human MCM8 in prereplication complex assembly by recruiting hcdc6 to chromatin. Mol. Cell. Biol. *25*, 1560–1568.

Yamamoto, K., Hirano, S., Ishiai, M., Morishima, K., Kitao, H., Namikoshi, K., Kimura, M., Matsushita, N., Arakawa, H., Buerstedde, J.M., et al. (2005). Fanconi anemia protein FANCD2 promotes immunoglobulin gene conversion and DNA repair through a mechanism related to homologous recombination. Mol. Cell. Biol. *25*, 34–43.

Yamamoto, K.N., Kobayashi, S., Tsuda, M., Kurumizaka, H., Takata, M., Kono, K., Jiricny, J., Takeda, S., and Hirota, K. (2011). Involvement of SLX4 in interstrand cross-link repair is regulated by the Fanconi anemia pathway. Proc. Natl. Acad. Sci. USA *108*, 6492–6496.

Yamashita, Y.M., Okada, T., Matsusaka, T., Sonoda, E., Zhao, G.Y., Araki, K., Tateishi, S., Yamaizumi, M., and Takeda, S. (2002). RAD18 and RAD54 cooperatively contribute to maintenance of genomic stability in vertebrate cells. EMBO J. *21*, 5558–5566.

Yoshida, K. (2005). Identification of a novel cell-cycle-induced MCM family protein MCM9. Biochem. Biophys. Res. Commun. *331*, 669–674.

Please cite this article in press as: Yan et al., A Ubiquitin-Binding Protein, FAAP20, Links RNF8-Mediated Ubiquitination to the Fanconi Anemia DNA Repair Network, Molecular Cell (2012), doi:10.1016/j.molcel.2012.05.026

Molecular Cell
Article

A Ubiquitin-Binding Protein, FAAP20, Links RNF8-Mediated Ubiquitination to the Fanconi Anemia DNA Repair Network

Zhijiang Yan,[1,9] Rong Guo,[1,9] Manikandan Paramasivam,[2] Weiping Shen,[1] Chen Ling,[1] David Fox III,[1] Yucai Wang,[3] Anneke B. Oostra,[4] Julia Kuehl,[5] Duck-Yeon Lee,[6] Minoru Takata,[7] Maureen E. Hoatlin,[8] Detlev Schindler,[5] Hans Joenje,[4] Johan P. de Winter,[4] Lei Li,[3] Michael M. Seidman,[2,*] and Weidong Wang[1,*]

[1]Laboratory of Genetics
[2]Laboratory of Molecular Gerontology
National Institute of Aging, National Institutes of Health, Baltimore, MD 21224, USA
[3]Department of Experimental Radiation Oncology and Department of Molecular Genetics, University of Texas M.D. Anderson Cancer Center, Houston, TX 77030, USA
[4]Department of Clinical Genetics, VU University Medical Center, 1081 BT Amsterdam, The Netherlands
[5]Department of Human Genetics, University of Wurzburg, D-97074 Wurzburg, Germany
[6]Biochemistry Core Facility, NHLBI, National Institutes of Health, Bethesda, MD 20892, USA
[7]Laboratory of DNA Damage Signaling, Department of Late Effect Studies, Radiation Biology Center, Kyoto University, Kyoto 606-8501, Japan
[8]Department of Biochemistry and Molecular Biology, Oregon Health and Science University, Portland, OR 97239, USA
[9]Co-first authors
*Correspondence: seidmanm@grc.nia.nih.gov (M.M.S.), wangw@grc.nia.nih.gov (W.W.)
DOI 10.1016/j.molcel.2012.05.026

SUMMARY

The Fanconi anemia (FA) protein network is necessary for repair of DNA interstrand crosslinks (ICLs), but its control mechanism remains unclear. Here we show that the network is regulated by a ubiquitin signaling cascade initiated by RNF8 and its partner, UBC13, and mediated by FAAP20, a component of the FA core complex. FAAP20 preferentially binds the ubiquitin product of RNF8-UBC13, and this ubiquitin-binding activity and RNF8-UBC13 are both required for recruitment of FAAP20 to ICLs. Both RNF8 and FAAP20 are required for recruitment of FA core complex and FANCD2 to ICLs, whereas RNF168 can modulate efficiency of the recruitment. RNF8 and FAAP20 are needed for efficient FANCD2 monoubiquitination, a key step of the FA network; RNF8 and the FA core complex work in the same pathway to promote cellular resistance to ICLs. Thus, the RNF8-FAAP20 ubiquitin cascade is critical for recruiting FA core complex to ICLs and for normal function of the FA network.

INTRODUCTION

DNA interstrand crosslinks (ICLs) are highly toxic lesions because they are absolute blocks to replication and transcription. In humans, the repair of ICLs requires a group of proteins in which mutations cause Fanconi anemia (FA), a genetic disorder characterized by developmental abnormalities, bone marrow failure, and cancer predisposition (Wang, 2007). FA patient cells display increased chromosome instability and cellular hypersensitivity in response to ICL-inducing agents. Fifteen genes defective in FA have been identified, and their products (FANC proteins) work with breast cancer susceptibility (BRCA) proteins to repair ICLs.

The FANC proteins can be classified into three groups. The first group includes the FA core complex, consisting of eight FANC proteins (FANCA, FANCB, FANCC, FANCE, FANCF, FANCG, FANCL, and FANCM) and four FA-associated proteins (FAAP100, FAAP24, MHF1, and MHF2) (Singh et al., 2010; Wang, 2007; Yan et al., 2010). In response to DNA damage or stalled replication, the core complex monoubiquitinates the second group of proteins, FANCD2 and FANCI, which form the "ID" complex, and its monoubiquitination is necessary for repair of ICLs (Knipscheer et al., 2009). The monoubiquitinated ID complex also redistributes to DNA damage sites on chromatin, where it colocalizes with the third group of FA proteins, FANCD1/BRCA2, FANCJ/BACH1/BRIP1, FANCN/PALB2. The monoubiquitinated ID complex may serve as a signal to recruit FANCP/SLX4 and nuclease FAN1 through interaction with their ubiquitin-binding zinc finger (UBZ) domains (Kratz et al., 2010; Liu et al., 2010; MacKay et al., 2010; Smogorzewska et al., 2010; Yamamoto et al., 2011).

All three groups of FANC proteins are recruited to ICLs in vivo and in vitro (Ben-Yehoyada et al., 2009; Knipscheer et al., 2009; Shen et al., 2009; Yan et al., 2010), but the recruitment mechanism is poorly understood. Recruitment of the FA core complex has been reported to depend on ATR kinase, RPA (which binds the ssDNA and activates ATR), and nucleotide excision repair proteins XPA and XPC (Ben-Yehoyada et al., 2009; Shen et al., 2009). Three DNA-binding components of the FA core complex (FANCM, MHF, and FAAP24) have also been suggested to bind directly to forks stalled by ICLs and recruit the complex (Huang et al., 2010; Yan et al., 2010).

Please cite this article in press as: Yan et al., A Ubiquitin-Binding Protein, FAAP20, Links RNF8-Mediated Ubiquitination to the Fanconi Anemia DNA Repair Network, Molecular Cell (2012), doi:10.1016/j.molcel.2012.05.026

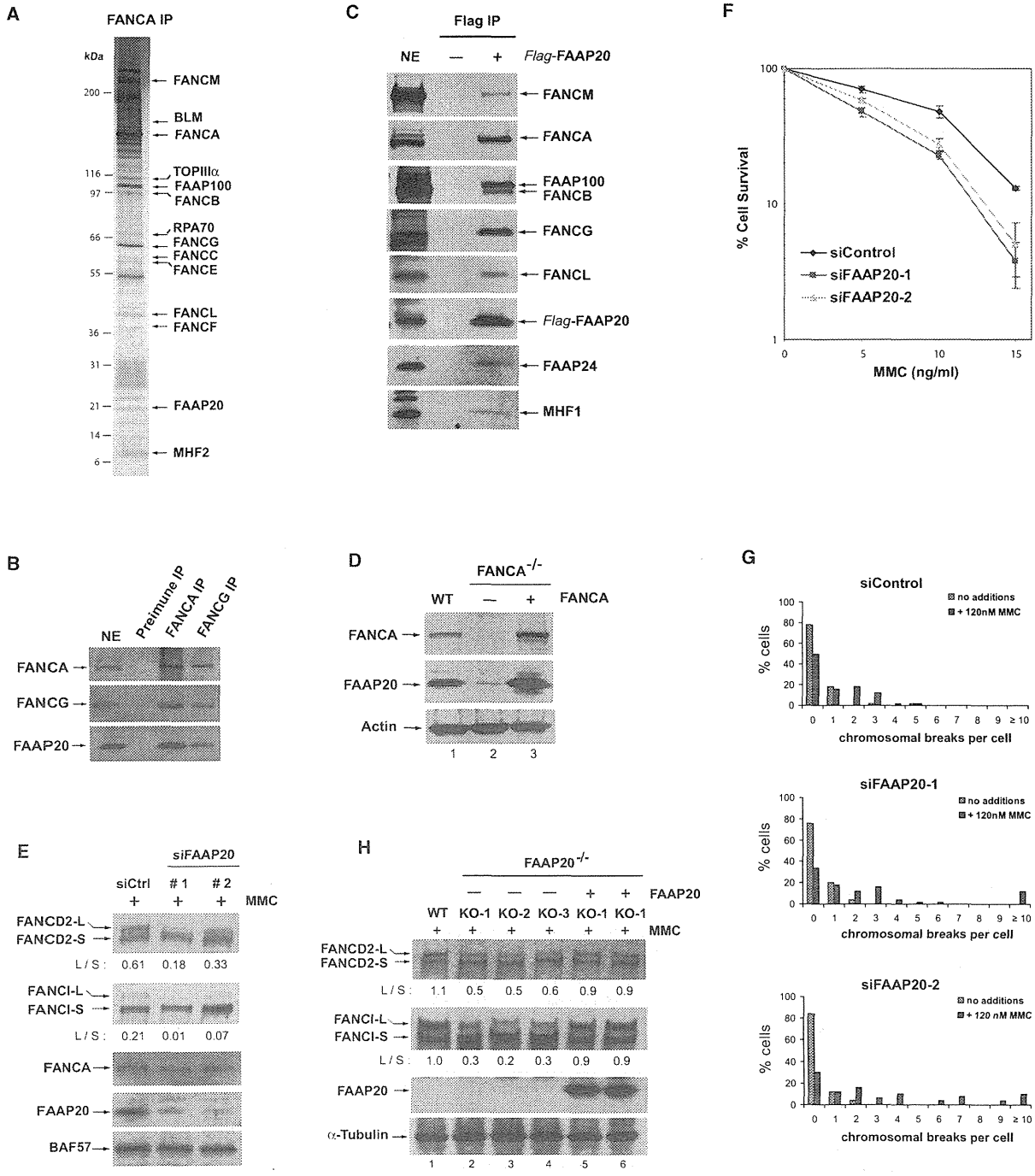

Figure 1. FAAP20 Is Required for Normal Activation of the FA Pathway and Cellular Resistance to ICLs

(A) A silver-stained gel showing that the complex purified by a FANCA antibody from HeLa nuclear extract contained FAAP20 and other components of FA core and BLM complexes. IP indicates immunoprecipitation.

(B) Immunoblotting shows that FAAP20 is present in the immunoprecipitates isolated from HeLa nuclear extract by FANCA or FANCG antibodies. Nuclear extract (NE) was used as a loading control.

(C) Immunoblotting shows that FAAP20 coimmunoprecipitated with FANCA and other FA core complex components from HeLa cells stably expressing Flag-tagged FAAP20, but not from untransfected HeLa cells. A Flag antibody was used in IP.

Please cite this article in press as: Yan et al., A Ubiquitin-Binding Protein, FAAP20, Links RNF8-Mediated Ubiquitination to the Fanconi Anemia DNA Repair Network, Molecular Cell (2012), doi:10.1016/j.molcel.2012.05.026

Here we show that FAAP20, a component of the FA core complex, preferentially binds lysine 63 (K63)- over lysine 48 (K48)-linked polyubiquitins in vitro. Both polyubiquitins have been observed in chromatin regions flanking DSBs and UV-induced DNA damage (Al-Hakim et al., 2010; Marteijn et al., 2009; Ulrich and Walden, 2010). RNF8 is the first E3 ubiquitin ligase that accumulates at damaged sites to build either K63- or K48-linked ubiquitin chains in damaged chromatin by working with different E2 ubiquitin-conjugating enzymes. Specifically, it can cooperate with UBC13 to promote K63-linked ubiquitination of H2A-type histones in response to DSBs, UV, and replication stress (Feng and Chen, 2012; Huen et al., 2007; Kolas et al., 2007; Mailand et al., 2007; Sy et al., 2011; Wang and Elledge, 2007). The ubiquitinated H2A then recruits a second E3 ligase, RNF168, which works with UBC13 to further elongate and spread K63-linked polyubiquitin chains. This enables assembly of downstream repair proteins at damaged chromatin via ubiquitin-mediated protein-protein interactions. In this study, we describe a ubiquitin signaling cascade that is initiated by RNF8-UBC13 and mediated by FAAP20. We show that this cascade is critical for recruitment of the FA core complex and FANCD2 to ICLs and also important for normal function of the FA network.

RESULTS

FAAP20 Is a Component of the FA Core Complex

We immunoprecipitated the FA core complex from HeLa nuclear extract with a FANCA antibody. Analyses of the immunoprecipitate by silver staining (Figure 1A) and mass spectrometry identified many known components of the FA core complex (FANCA, FANCB, FANCC, FANCE, FANCF, FANCG, FANCL, FANCM, FAAP100, and MHF2) and the BLM complex (BLM, TOPIIIα, and RPA70). The results confirmed the association of the FA core complex and BLM complex in a supercomplex, BRAFT (Meetei et al., 2003). We also identified a 20 kDa polypeptide as LOC199990 (C1ORF86), an uncharacterized protein. We renamed it as FAAP20 (for FA-associated protein 20 kDa).

Immunoblotting showed that a FAAP20 antibody recognized the corresponding polypeptide in the FA core complex immunoprecipitated with either anti-FANCA or FANCG antibodies (Figure 1B). In a reciprocal immunoprecipitation, FAAP20-associated polypeptides isolated by a Flag antibody from the extract of HeLa cells stably expressing Flag-tagged FAAP20 contained many FA core complex components (Figure 1C). Additionally, the profile of FAAP20 on gel filtration chromatography overlapped with those of several FA core complex components (see Figure S1A available online). Notably, the profile of FAAP20 was coincidental with those of FANCA and FANCG, arguing that these three proteins are likely present in a subcomplex.

The level of FAAP20 was significantly reduced in cells derived from a FANCA patient compared to that of cells from a healthy individual (Figure 1D, lanes 1 and 2), and this FAAP20 level was restored by reinduction of exogenous FANCA (Figure 1D, lanes 2 and 3). These data indicate that the stability of FAAP20 is dependent on FANCA, suggesting that FAAP20 could interact with FANCA in the FA core complex.

FAAP20 Is Required for Normal Activation of the FA Pathway and Cellular Resistance to ICLs

A key function of the FA core complex is to monoubiquitinate FANCD2 and FANCI in response to DNA damage. HeLa cells depleted of FAAP20 by two different siRNAs displayed reduced levels of monoubiquitinated FANCD2 and FANCI in response to mitomycin C (MMC) (Figure 1E and Figure S1B), indicating that FAAP20 is a functional component of the core complex. The reduced ubiquitination was not due to inability of these cells to enter S phase, because the S phase population in cells depleted by siFAAP20-2 oligo was larger than that of cells treated with a control siRNA (Figure S1C). The FAAP20-depleted HeLa cells exhibited increased sensitivity to MMC (Figure 1F) as well as increased MMC-induced chromosomal breaks (Figure 1G). These are all characteristics of cells deficient in the FA core complex, suggesting that FAAP20 is important for normal function of the FA pathway and for cellular resistance to ICLs.

The FAAP20-depleted HeLa cells had a modestly reduced level of FANCA compared to cells treated with a control oligo (Figure 1E and Figure S1B), again consistent with a need for FAAP20 for optimal stability of FANCA.

We further investigated the role of FAAP20 by inactivating this gene in chicken DT40 cells (Figures S1D–S1F). The levels of both monoubiquitinated FANCD2 and FANCI were reduced in three independent clones of *FAAP20*$^{-/-}$ DT40 cells when compared to wild-type cells (Figure 1H, lanes 1–4; and Figure S1G), and these were restored by reintroduction of human FAAP20 into these cells (Figure 1H, lanes 1, 2, 5, and 6). The results are consistent with the data from HeLa cells that showed a requirement of FAAP20 for optimal monoubiquitination of FANCD2 and FANCI after DNA damage.

The *FAAP20*$^{-/-}$ DT40 cells did not exhibit significant sensitivity to cisplatin, which can induce ICLs (data not shown). This

(D) Immunoblotting shows the level of FAAP20 in lysates of lymphoblastoid cells from a healthy individual (WT), a FANCA patient (*FANCA*$^{-/-}$), and the patient cell line complemented by expression of exogenous FANCA.

(E) Immunoblotting shows that HeLa cells depleted of FAAP20 by two different siRNAs have reduced levels of monoubiquitinated FANCD2 and FANCI in the presence of 60 ng/ml MMC for 20 hr. A nontargeting siRNA was used as a control (siCtrl). "L" (long) and "S" (short) represent monubiquitinated and non-ubiquitinated forms, respectively. The ratio between long and short forms (L/S) was obtained by using KODAK Molecular Imaging Software and is shown below the blots.

(F) Clonogenic survival assays of HeLa cells depleted of FAAP20 by two different siRNAs following the treatment with MMC. The mean surviving percentages with standard error of the mean (SEM) from three independent experiments are shown.

(G) MMC-induced chromosomal aberrations in HeLa cells depleted of FAAP20 by two different siRNAs. Percentages of metaphases with and without aberrations after MMC treatment were compared between siControl and siFAAP20 cells using a two-sample Chi^2 test. p values for the differences between siFAAP20-1, siFAAP20-2 and siControl were 0.05 and 0.02, respectively.

(H) Immunoblotting shows the levels of FANCD2 and FANCI in lysates from various DT40 cells (wild-type [WT], *FAAP20*$^{-/-}$ cells of three independent clones [KO-1, KO-2, and KO-3], and *FAAP20*$^{-/-}$ cells complemented with human FAAP20). Cells were treated with 500 ng/ml MMC for 6 hr (see also Figure S1).

Please cite this article in press as: Yan et al., A Ubiquitin-Binding Protein, FAAP20, Links RNF8-Mediated Ubiquitination to the Fanconi Anemia DNA Repair Network, Molecular Cell (2012), doi:10.1016/j.molcel.2012.05.026

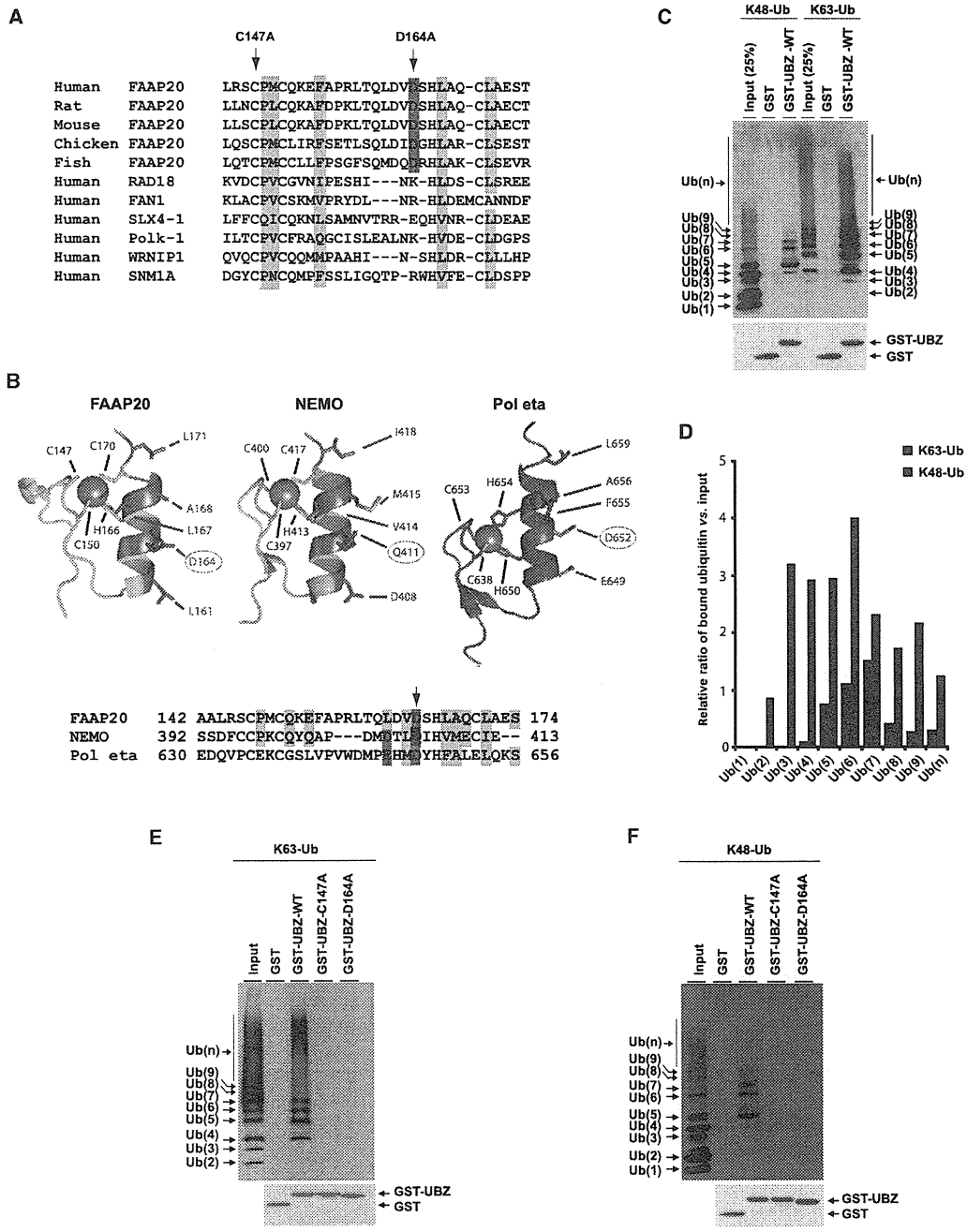

Figure 2. The UBZ Domain of FAAP20 Preferentially Binds K63-Linked over K48-Linked Polyubiquitin Chains In Vitro

(A) Sequence alignment of the UBZ domains of FAAP20 orthologs and several other proteins. Conserved residues of the zinc finger are marked yellow. A critical aspartate residue for ubiquitin binding is marked red. Other identical and similar residues are marked green. Two point mutants of human FAAP20 are indicated.

(B) (Top panel) A homology model to compare the UBZ domains of human FAAP20, NEMO, and Pol eta. Hydrophobic residues (green), acidic residues (red), polar uncharged (magenta), and the zinc coordinating residues (blue) are shown as sticks. (Bottom panel) Sequence alignment of the UBZ domains. A critical residue at the ubiquitin-binding interface is indicated by an arrow.

(C) GST pull-down coupled with immunoblotting shows the binding of both K48- and K63-linked polyubiquitin chains by a GST fusion protein containing the wild-type (WT) UBZ domain of FAAP20 (GST-UBZ-WT), but not by GST protein alone.

may not be a surprise, because DT40 cells deficient in FANCA or FANCG (which may interact more directly with FAAP20 in a subcomplex; Figure S1A) are not very sensitive to crosslinking agents, unlike DT40 cells deficient in FANCL or FANCC, which are highly sensitive (Takata et al., 2009). It should be mentioned that cell survival is affected not only by the FA network but also by other pathways; and measuring FANCD2 monoubiquitination and foci formation is a more direct readout for the FA network.

No FA Patients Have Yet Been Found with Mutations in *FAAP20*

We screened unclassified FA patients, which lacked a defect in any of the known FA genes, for *FAAP20* mutations by both immunoblotting and exon sequencing but found no patient with a *FAAP20* defect (data not shown).

FAAP20 Contains a UBZ-Type Ubiquitin-Binding Domain

FAAP20 orthologs are found in vertebrates, but not in invertebrates and yeast (Figure S2A). This feature of FAAP20 is shared by most FA core complex components, suggesting that the genes encoding them may have coevolved.

Alignment of FAAP20 sequences revealed a highly conserved zinc finger domain (Figure S2A) similar to the UBZ domain found in other DNA repair proteins, including FAN1 and FANCP/SLX4 (Figure 2A). Atomic absorption analyses of a recombinant GST-fusion protein containing the UBZ domain of FAAP20 confirmed the presence of a Zn atom in the wild-type protein (GST-UBZ-WT), but not in a point mutant carrying a Cys-to-Ala substitution (GST-UBZ-C147A) (Figure 2A and Figure S2B).

The UBZ domain of FAAP20 bound ubiquitin-conjugated agarose beads in a pull-down assay (Figure S2C). In contrast, neither GST protein alone nor two GST-fusion proteins carrying point mutations in the UBZ domain (C147A and D164A, respectively) bound to ubiquitin beads (Figure 2A and Figure S2C). These data indicate that the UBZ domain of FAAP20 is indeed a ubiquitin-binding domain.

Of the two UBZ mutations (Figure 2A), the C147A substitution inactivates Zn binding (Figure S2B) and disrupts the tertiary structure of the domain. The D164A substitution mimics a similar mutation in the UBZ domains of Pol eta (D652) and Nemo (Q411), which disrupts the ubiquitin-binding surface without affecting tertiary structure (Figures 2A and 2B) (Bomar et al., 2007; Cordier et al., 2009). As expected, the D164A mutant retained the Zn atom in the structure (Figure S2B). Thus, our findings that the D164A mutant lost ubiquitin-binding activity suggest that the ubiquitin interface of the FAAP20 UBZ domain may be similar to that in other UBZ domains.

The UBZ Domain of FAAP20 Binds Both K48- and K63-Linked Polyubiquitin Chains

Proteins can be modified by either mono- or polyubiquitins linked through different lysine (K) residues, with different ubiquitin isoforms representing distinct signals for their host proteins. We found that a GST fusion protein containing the UBZ domain of FAAP20 bound both K48- and K63-linked polyubiquitin chains but had no detectable binding for monoubiquitin (Figures 2C and 2D). As controls, GST-fusion proteins containing the UBZ domain with either C147A or D164A mutations had no binding activity for either form of polyubiquitin (Figures 2E and 2F). The results suggest that FAAP20 can recognize both K48- and K63-linked polyubiquitin, but not monoubiquitin.

We quantified the immunoblot images for each ubiquitin linkage and calculated the ratio between levels of the bound ubiquitin versus those of the input (Figure 2D). The results showed that the ratio for each K63-linked chain is consistently higher than that for the respective K48-linked chain, indicating that the FAAP20-UBZ domain preferentially binds K63-linked chains.

The Ubiquitin-Binding Activity Is Crucial for FAAP20 Recruitment to ICLs

Two FA core complex components, FANCM and MHF1, are recruited to ICLs induced by laser-activated psoralen (Yan et al., 2010). Using the same method, we observed recruitment of GFP-tagged FAAP20 at ICLs within minutes upon laser activation (Figure 3A). Notably, no recruitment was detected for the GFP-FAAP20-D164A mutant that lacks ubiquitin-binding activity (Figures 3B and 3C).

We also performed eChIP, a chromatin-IP-based assay that detects the recruitment of the FA core complex to an ICL on a nonreplicating episomal plasmid (Shen et al., 2009). Flag-FAAP20 was recruited to the ICL, but the Flag-FAAP20-D164A mutant was not (Figure 3D and Figure S3A). These data indicate that FAAP20 is recruited to ICLs through the ubiquitin-binding activity of its UBZ domain.

K63-Linked Polyubiquitin Generated by RNF8-UBC13 Signals FAAP20 Recruitment

RNF8 is the first E3 ligase that accumulates at damaged DNA to build either K63- or K48-linked ubiquitin chains in the surrounding chromatin. Because both products of RNF8 can be bound by FAAP20, we investigated whether RNF8-dependent ubiquitination recruits FAAP20 to damaged sites. The accumulation of GFP-FAAP20 at ICLs was abolished in HeLa cells depleted of RNF8 by two different siRNAs (Figures 3E and 3F, and Figure S3B). These data suggest that RNF8 and FAAP20 constitute a ubiquitin signaling cascade (RNF8-FAAP20 cascade) in which RNF8-mediated ubiquitination is a signal for FAAP20 recruitment.

K63-linked polyubiquitins often recruit other proteins through ubiquitin-mediated interactions, whereas K48-linked chains target substrates for proteolytic degradation. To examine whether K63-linked polyubiquitin is the signal for FAAP20 recruitment, we depleted UBC13, the ubiquitin-conjugating

(D) A graph shows the ratio between levels of the bound ubiquitin versus those of input as reported in (C). The immunoblotting in (C) was quantified by KODAK Molecular Imaging Software. Notably, for each ubiquitin isoform, binding to K63 linked chains is consistently stronger than K48 chains.
(E and F) GST pull-down coupled with immunoblotting shows the binding of K63- or K48-linked polyubiquitin by wild-type (WT) UBZ domain, but not by GST-UBZ mutants (C147A and D164A, respectively) (see also Figure S2).